Available online at www.sciencedirect.com
SCIENCE DIRECT®
PERGAMON
Deep-Sea Research I 50 (2003) 781–807
DEEP-SEA RESEARCH PART I
www.elsevier.com/locate/dsr

Biogenic fluxes in the Cariaco Basin: a combined study of sinking particulates and underlying sediments

Miguel A. Goñi[a,*], Heather L. Aceves[a], Robert C. Thunell[a], Eric Tappa[a], David Black[a,1], Yrene Astor[b], Ramon Varela[b], Frank Muller-Karger[c]

[a] *Department of Geological Sciences, University of South Carolina, Earth and Water Sciences Building, 302 700, Sumter Street, Columbia, SC 29208, USA*

[b] *Estacion de Investigaciones Marinas de Margarita, Fundacion La Salle de Ciencias Naturales, Aptdo. 144, Porlamar 6301, Venezuela*

[c] *Department of Marine Science, University of South Florida, St. Petersburg, FL 33701, USA*

Received 23 July 2002; received in revised form 31 December 2002; accepted 11 March 2003

Abstract

The fluxes of total mass, organic carbon (OC), biogenic opal, calcite ($CaCO_3$) and long-chain C_{37} alkenones (ΣAlk_{37}) were measured at three water depths (275, 455 and 930 m) in the Cariaco Basin (Venezuela) over three separate annual upwelling cycles (1996–1999) as part of the CARIACO sediment trap time-series. The strength and timing of both the primary and secondary upwelling events in the Cariaco Basin varied significantly during the study period, directly affecting the rates of primary productivity (PP) and the vertical transport of biogenic materials. OC fluxes showed a weak positive correlation ($r^2 = 0.3$) with PP rates throughout the 3 years of the study. The fluxes of opal, $CaCO_3$ and ΣAlk_{37} were strongly correlated ($0.6 < r^2 < 0.8$) with those of OC. The major exception was the lower than expected ΣAlk_{37} fluxes measured during periods of strong upwelling. All sediment trap fluxes were significantly attenuated with depth, consistent with marked losses during vertical transport. Annually, strong upwelling conditions, such as those observed during 1996–1997, led to elevated opal fluxes (e.g., 35 g m^{-2} yr^{-1} at 275 m) and diminished ΣAlk_{37} fluxes (e.g., 5 mg m^{-2} yr^{-1} at 275 m). The opposite trends were evident during the year of weakest upwelling (1998–1999), indicating that diatom and haptophyte productivity in the Cariaco Basin are inversely correlated depending on upwelling conditions.

The analyses of the Cariaco Basin sediments collected via a gravity core showed that the rates of OC and opal burial (10–12 g m^{-2} yr^{-1}) over the past 5500 years were generally similar to the average annual water column fluxes measured in the deeper traps (10–14 g m^{-2} yr^{-1}) over the 1996–1999 study period. $CaCO_3$ burial fluxes (30–40 g m^{-2} yr^{-1}), on the other hand, were considerably higher than the fluxes measured in the deep traps ($\sim$10 g m^{-2} yr^{-1}) but comparable to those obtained from the shallowest trap (i.e. 38 g m^{-2} yr^{-1} at 275 m). In contrast, the burial rates of ΣAlk_{37} (0.4–1 mg m^{-2} yr^{-1}) in Cariaco sediments were significantly lower than the water column fluxes measured at all depths (4–6 mg m^{-2} yr^{-1}), indicating the large attenuation in the flux of these compounds at the sediment–water interface. The major trend throughout the core was the general decrease in all biogenic fluxes with depth, most likely due to post-depositional in situ degradation. The major exception was the relatively low opal fluxes ($\sim$5 g m^{-2} yr^{-1}) and elevated ΣAlk_{37} fluxes ($\sim$2 mg m^{-2} yr^{-1}) measured in the sedimentary interval corresponding to 1600–2000 yr BP. Such

*Corresponding author. Tel.: +1-803-777-3550; fax +1-803-777-6610.
E-mail address: goni@geol.sc.edu (M.A. Goñi).
[1] Current address: Department of Geology, 252 Buchtel Common, University of Akron, Akron, OH 44325-4101, USA.

0967-0637/03/$ - see front matter
doi:10.1016/S0967-0637(03)00060-8

compositions are consistent with a period of low diatom and high haptophyte productivity, which based on the trends observed from the sediment traps, is indicative of low upwelling conditions relative to the modern day.

Keywords: Biogenic fluxes; Organic carbon; Biogenic opal; Alkenones; Sediment traps; Marine sediments; Venezuela; Cariaco Basin; 10°30′N, 64°40′W

1. Introduction

The chemical and micropaleontological signatures preserved in marine sediments have long been used to reconstruct past oceanographic and climatic conditions in the world's oceans. Sediments underlying anoxic water columns are especially useful because the absence of oxygen and macro-fauna often results in undisturbed records with a high degree of preservation. Among these, the sediments from the deeper parts of the Cariaco Basin display extensive varved sections and are characterized by relatively high accumulation rates due to seasonally alternating high surface primary productivity (PP) and abundant supply of lithogenic material from the proximal land masses. These characteristics provide an exceptional archive of past conditions in the tropics that has been exploited by numerous investigators to produce high-quality and high-resolution records of climate change (e.g., Overpeck et al., 1989; Hughen et al., 1996a, b, 2000; Haug et al., 1998; Black et al., 1999; Peterson et al., 1991, 2000; Werne et al., 2000). In order to better reconstruct past climate, however, an improved understanding of how the conditions in the surface ocean and euphotic zone are "recorded" in the underlying sediments of the Cariaco Basin is needed.

As part of this overall objective, we investigated how upwelling, water column stratification, and PP control the production, composition, and vertical transport of biogenic materials in the water column and to the surface sediments of the Cariaco Basin. For this purpose, we analyzed sediment trap samples collected at three depths during a 3-year (1997–1999) period as part of the CArbon Retention In A Colored Ocean (CARIACO) time-series study (Muller-Karger et al., 2001). In this study, we focused on the concentrations and fluxes of organic carbon (OC), opal, $CaCO_3$ and long-chain alkenones, the last of which are compounds uniquely synthesized by haptophyte algae including coccolithophores such as *Emiliania huxleyi* and *Gephyrocapsa oceanica* (e.g., Volkman et al., 1980, 1995; Marlowe et al., 1984). Coupled with monthly cruises, which provided simultaneous observations of the euphotic zone, these samples represent an excellent opportunity to assess how the primary signals produced in the euphotic zone are transferred to the sediments.

In order to compare water column flux estimates to those from the sediment record, we analyzed samples from a gravity core collected from the study area. These sediments were analyzed for the same biogenic materials (OC, opal, $CaCO_3$ and long-chain alkenones) determined in the sediment trap samples. Coupled with estimates of sedimentation rates, these data were used to calculate biogenic burial fluxes in the study area over the past 6000 years.

2. Background

2.1. Study area

The Cariaco Basin (Fig. 1) is a 1400-m deep depression off the Venezuelan central coast composed of two sub-basins that are separated by a saddle that rises up to 900 m. The basin, which acts as natural sediment trap within the continental shelf (Richards, 1975; Lidz et al., 1969), is connected with the surface Atlantic Ocean above a shallow (100 m) sill and through two channels, the 135 m deep Canal de la Tortuga located to the northeast and the narrower and

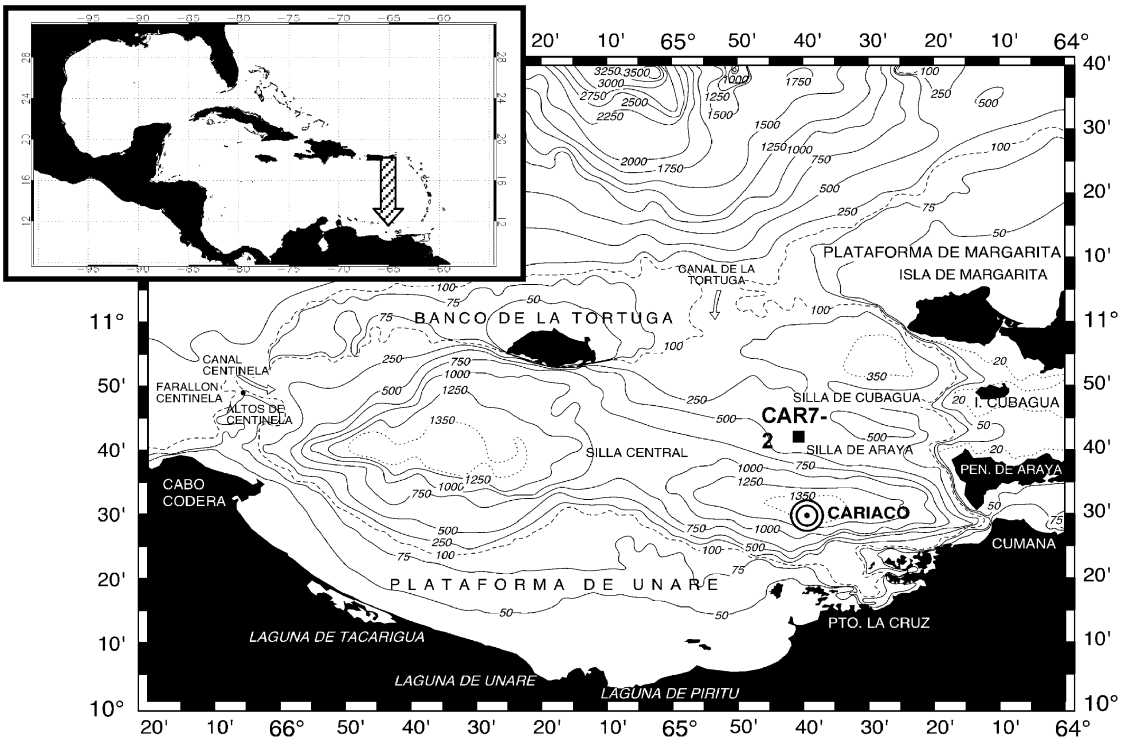

Fig. 1. Map of the Cariaco Basin with the locations of the sediment trap (CARIACO) and gravity core (CAR7-2) sites.

deeper (146 m) Canal Centinela. The sill and relatively shallow channels restrict the circulation of deep water through the Cariaco Basin. Because of this restricted circulation, the decomposition of organic material sinking from the surface has led to the complete consumption of dissolved oxygen within the bottom waters, resulting in anoxia below approximately 275 m (Deuser, 1973).

Upwelling, induced by winds and western boundary currents, drives the annual production cycle in the Cariaco Basin (Herrera and Febres-Ortega, 1975; Muller-Karger and Aparicio-Castro, 1994). As the latitude of the Intertropical Conversion Zone (ITCZ) changes from its northern to its southern most position, strong easterly/northeasterly trade winds develop from December to April. Surface Ekman transport induced by these steady winds causes an upward migration of the thermocline along the east–west oriented continental margin off the Venezuelan coast, bringing nutrients from deeper waters. During the summer/fall rainy season, the ITCZ migrates north, causing winds to become weaker and upwelling to greatly diminish or cease. The source of the upwelled water in the Cariaco region is Subtropical Underwater, which in this part of the Caribbean margin lies shallower than 150 m and is characterized by a salinity of 36.85 and a nitrate concentration of 5–10 μM (Morrison and Smith, 1990; Morrison and Nowlin, 1982).

2.2. CARIACO time-series program

In November of 1995, the CARIACO program started a systematic study of the carbon cycle in the Cariaco Basin (Muller-Karger et al., 2001). The program is composed of investigators from several US institutions (including University of South Florida, State University of New York Stony Brook, and University of South Carolina) as well as several institutions from Venezuela (including Fundacion La Salle de Ciencias Naturales

and Instituto Ocenaografico de la Universidad de Oriente). Monthly cruises to the study site (10°30′N, 64°40′W) measure basic hydrographic properties (temperature, salinity) and collect water samples for nutrient, alkalinity, pH, dissolved oxygen, chlorophyll, and PP analyses, as well as studies of bacterial metabolism and productivity. Four sediment traps located at depths of 275, 455, 930 and 1255 m have been in place since the start of the project, collecting sinking particles at bi-weekly intervals (Thunell et al., 2000). These samples have been analyzed for major components (OC, nitrogen, biogenic opal, calcium carbonate) and organic biomarkers in order to estimate biogenic fluxes. Satellite observations (AVHRR, OCTS, SeaWiFS) provide continual data on the conditions in the surface ocean. An overview of the extent of activities of the CARIACO program is available at the CARIACO web site (http://imars.marine.usf.edu), which also serves as a data repository.

The intense observations that have been carried out as part of the CARIACO time-series have provided new insights regarding the hydrography, productivity, and geochemistry of the Cariaco Basin (Astor et al., 2003; Muller-Karger et al., 2001; Scranton et al., 2001; Taylor et al., 2001; Thunell et al., 1999, 2000; Walsh et al., 1999). These findings indicate that while the upwelling regime in the Cariaco Basin responds to wind changes in the southern Caribbean Sea, the upwelling process is more complex than previously understood, as it is affected by regional ocean circulation events such as eddies transiting the southern Caribbean from east to west. Upwelling controls PP in surface waters, but lateral intrusions of Caribbean Sea water into the Cariaco Basin also play an important role in regulating the biogenic export from the surface and redox conditions in the basin interior (Astor et al., 2003; Scranton et al., 2001).

In this paper, we present hydrographic and sediment trap composition data for three annual upwelling cycles, November–October of 1996–1997, 1997–1998 and 1998–1999. Part of the hydrographic data (1997 and 1998) and carbon, opal, and carbonate flux data (1997) have been presented elsewhere (Astor et al., 2003; Muller-Karger et al., 2001). However, the biomarker flux data as well as the sediment compositions are new. Here, we discuss these observations and results in the context of paleoceanographic applications.

3. Methods

3.1. Sample collection

Cruises to the study site were conducted every month throughout the study period (November 1996–October 1999) by the Research Vessel *Hermano Ginés* (R./V. *H. Ginés*), operated by Fundación La Salle de Ciencias Naturales (FLASA) from the Estación de Investigaciones Marinas Margarita (EDIMAR) located on Isla Margarita. During each cruise, a Seabird^{TM} rosette was used to collect water samples at eight depth intervals (1–2, 6–8, 14–16, 24–26, 34–36, 54–56, 74–76 and 98–100 m) that were used for PP measurements. A rosette-mounted CTD was used to obtain continuous profiles of conductivity and temperature at 1-m intervals for the top 100 m of the water column.

A single mooring containing four automated sediment traps (Honjo and Doherty, 1988) was deployed in the eastern sub-basin of the Cariaco Basin (10°30′N, 64°40′W) at a depth of approximately 1400 m (Fig. 1) as described by Thunell et al. (2000). The traps were placed at four different depths: trap A at 275 m, just above the oxic/anoxic interface, trap B at 455 m, trap C at 930 m and trap D at 1255 m. The 13 rotating cups were programmed to collect samples at 2-week intervals. Each deployment lasted 6 months and a buffered formalin solution was placed in each trap cup prior to deployment in order to minimize post-depositional degradation of the organic matter. After collection, samples were stored in sealed containers and kept refrigerated until analyses. Prior to analyses, samples were thoroughly washed with distilled water to remove excess formalin and carefully examined under the microscope to remove swimmers that are not part of the particle flux (Thunell et al., 2000). Samples were dried in either an oven (50°C) or a freeze drier and weighed to obtain the total mass (TM) flux ($g\,m^{-2}\,d^{-1}$).

The weight percent contents of organic carbon (%OC), biogenic opal (%Opal), and calcite (%$CaCO_3$) were determined for all sediment trap samples. Because of sample availability constraints, the concentrations of long-chain C_{37} alkenones (ΣAlk_{37}) were generally measured in every other sediment trap sample over the 3-year study period.

In November 1998, a 220 cm long gravity core (CAR7-2) was collected from the location identified in Fig. 1 (10°39.055′N, 64°39.595′W, 449 m water depth). This site was chosen because it is located well below the oxycline in a relatively flat portion of the north side of the eastern basin (Silla de Araya), which minimizes the occurrence of turbidites. The core site is located between the depths of traps B and C, so that fluxes from these traps should provide direct constraints to those measured in the sediments. Once collected, the gravity core was kept upright and covered, while the top was allowed to air-dry and consolidate for 48 h. The core was split lengthwise and the two halves sub-sampled at different frequencies. One half of the core was sub-sampled at 0.5 cm intervals throughout its length and selected horizons were used for geochemical analyses. The other half of the core was sub-sampled at consecutive millimeter intervals over its entire length for planktic foraminifera population determinations and stable oxygen and carbon isotope analyses. We used this half of the core to derive an age model (Black et al., 2001) based on accelerator mass-spectrometry (AMS) ^{14}C dates on monospecific samples of the planktic foraminifer *Globigerina bulloides*.

3.2. Analytical techniques

PP measurements were conducted at the eight water depths by a modified $NaH^{14}CO_3$ uptake assay as described by Muller-Karger et al. (2001). Carbon uptake calculations followed standard formulation outlined in the Joint Global Ocean Flux Study (United Nations Educational, Scientific, and Cultural Organization, 1994). The daily productivity was obtained by applying a photoperiod scaling factor based on the shipboard photosynthetically active radiation photometer sensor as reference (Muller-Karger et al., 2001). The productivity measurements obtained by this approach have been shown to agree very well (within ~10%) with the estimates derived from coupled biological–physical models of carbon and cycling for the area (Walsh et al., 1999).

Weight percent organic carbon (%OC) was determined after removal of carbonates by combustion in a Perkin-Elmer 2400 Elemental Analyzer based on the procedure of Froelich (1980) as described by Goñi et al. (2001). The weight percent of biogenic silica (%Opal) was determined according to the method of Mortlock and Froelich (1989). Total inorganic carbon and the associated calcium carbonate contents (%$CaCO_3$) were determined by the automated acidification procedure of Ostermann et al. (1990). The average error of the %OC, %Opal, and %$CaCO_3$ determinations were 2%, 6% and 4% of the measured value, respectively.

The concentrations of the two major long-chain alkenones, di- and tri-unsaturated methyl C_{37} ketones (37:2Me and 37:3Me, respectively), were determined by the procedure of Rosell-Melé et al. (1995) as described by Goñi et al. (2001). Briefly, known amounts of sample were extracted by sonication in triplicate with a 3:1 dichloromethane/methanol solution. Prior to the extraction step, hexatriacontane was added as a recovery standard. The initial extracts were cleaned using preconditioned solid phase extraction columns and eluted with a solution of dichloromethane with 1% methanol. Prior to gas chromatographic (GC) analyses, the extracts were silylated overnight, dried and re-dissolved in dichloromethane. GC analyses were carried out on a Hewlett-Packard 6890 GC equipped with on-column injector and flame ionization detector (FID). The concentrations of the long-chain alkenones were determined assuming the same FID response factor as the hexatriacontane standard. All compound identities were confirmed by co-injection of synthetic standards and by mass spectrometric analyses with a Varian 2000 Saturn ion trap GC-MS. The error in the combined concentrations of the C_{37} alkenones (ΣAlk_{37}) ranged from 5% to 15% of the measured value, with the largest variability being associated with those samples with lowest concentrations.

4. Results

4.1. Oceanographic conditions in the upper ocean

Overall, there were significant differences in the extent of upwelled water that reached the euphotic zone during this 3-year period (Fig. 2). For example, in the 1996–1997 cycle, the main upwelling event started somewhat late (December 1996) but the shoaling of the cool waters was fast and intense, with the 22°C isotherm reaching 10 m in March 1997 (Fig. 2a). The upwelling period this year was relatively long lasting from December to April. This main upwelling period, which typically occurs in the Cariaco Basin during the months of November–March, consistently follows the seasonal increase in local wind speeds by periods of 1–2 weeks (Astor et al., 2003; Muller-Karger et al., 2001; note that Muller-Karger et al., 2001, erroneously concluded that winds lagged sea surface temperature because of flawed wind data collected at the regional airport on Margarita Island, Venezuela).

In 1997, the stratification of the water column started in April with the warming of the surface layers, but it was cut short by a second intense

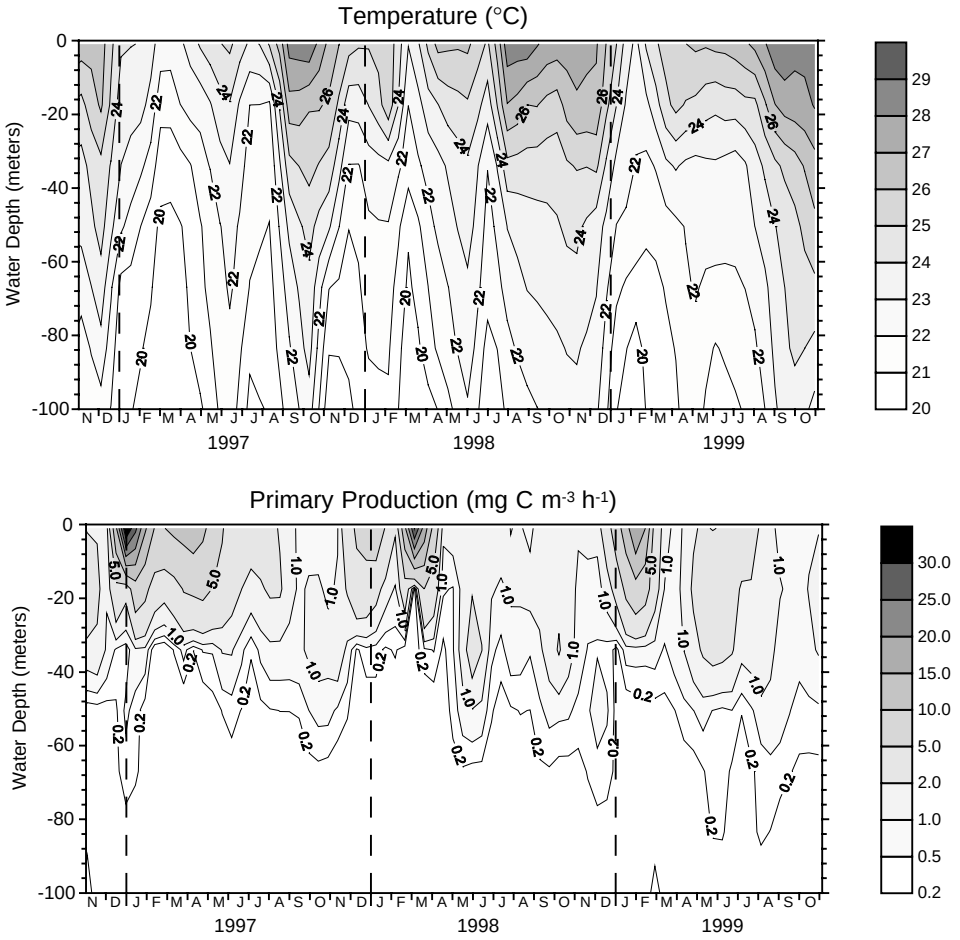

Fig. 2. Plots of (a) temperature and (b) PP for the top 100 m of the water column at the study site. Data based on the monthly hydrocasts performed from the R./V. *H. Ginés*. Temperature data were averaged at 1-m intervals from the continuous CTD profiles. PP measurements based on $NaH^{14}CO_3$ uptake were carried out with water samples collected at eight depth intervals (1–2, 6–8, 14–16, 24–26, 34–36, 54–56, 74–76 and 98–100 m). Dates of the hydrocasts and average values presented in Table 1.

upwelling event that started in June and lasted until mid-August, during which the 22°C isotherm reached the 20 m depth (Fig. 2a). This secondary upwelling event coincides with the maximum local winds in the Cariaco Basin, and originates from the shoaling of Cariaco Basin waters rather than being an extension of the regional upwelling that occurs earlier in the season (Astor et al., 2003). Thermal stratification was reestablished in late August, reaching temperatures of 28°C in the near surface in September and October 1997 (Fig. 2a).

The 1997–1998 period coincided with an El Niño event (Chavez et al., 1999) and was characterized by significantly lower winds (Astor et al., 2003). Upwelling this year was much less pronounced than in the previous annual cycle. The shoaling of deep water started earlier, October 1997, but it was disrupted in December when a stratified pool of warmer water developed and persisted until February 1998 (Fig. 2a). Upwelling resumed in late February 1998 and lasted until late March, but the overall result was a much less pronounced cooling of the surface ocean, with the 22°C isotherm reaching the 20 m depth only for a brief period that year (Fig. 2a). As with the previous year, a secondary upwelling event also occurred in early June 1998, but it was considerably shorter and less intense than the one in 1997, lasting only until July with the 22°C isotherm shoaling only to 40 m. The period of stratification that followed this secondary upwelling was extensive and lasted until November 1998, with maximum temperatures exceeding 28°C at the surface during August and September.

The weakest upwelling and the longest period of stratification and warming of the upper water column occurred during 1999. Upwelling started more gradually than in previous years in mid-November 1998 and ended in the following February. The event was not as intense as in other years, with the 22°C isotherm reaching only 40 m depth at the end of this period. Thermal stratification of the water column started early and, unlike the previous 2 years, the secondary upwelling event was very small causing only a slight "bulge" of the isotherms, with the 22°C isotherm reaching a depth of only 60 m (Fig. 2a). The warming of the surface waters this year was more extensive than previous years, with sea surface temperatures of 26°C by late April and greater than 28°C by early September. The pool of warm water (>28°C) extended down to almost 20 m in October 1999 (Fig. 2a).

In order to summarize the upwelling-stratification cycles in the Cariaco Basin, we chose the depth-integrated temperature for the upper 25 m of the water column ($T_{0-25\,m}$) as a parameter. Accordingly, based on the trends in Fig. 2, upwelling periods are defined by $T_{0-25\,m} < 24.5$°C, whereas non-upwelling, stratification periods are characterized by $T_{0-25\,m} > 24.5$°C (Table 1). The seasonal and annual trends in $T_{0-25\,m}$ (Table 1) confirm the patterns presented above. In the 1996–1997 cycle, the annual average in $T_{0-25\,m}$ (24.3°C) was almost 1° cooler than the mean for the 1997–1998 cycle (25.1°C), which in turn was cooler than the annual mean for 1998–1999 (25.5°C). Overall, there was a 1.2°C warming of the upper water column from 1997 to 1999 (Table 1) that resulted from differences in regional circulation and local wind stress (Astor et al., 2003; Muller-Karger et al., 2001).

4.2. Seasonal and inter-annual trends in primary production

The distribution of primary production (PP) rates (in units of mg C m^{-3} h^{-1}) throughout the surface waters of the Cariaco Basin is illustrated in Fig. 2b. PP rates generally followed the shoaling of deep water, with the highest rates typically measured during the main upwelling periods between December and March of each year. Lower PP measurements were obtained during the secondary upwelling events in the summer months whereas, in general, the lowest rates were measured during periods of stratification (Fig. 2b). However, there were significant differences in the distribution and magnitude of phytoplankton productivity among the three annual upwelling cycles. For example, in the first year of the study, which was characterized by the strongest upwelling, we observed high levels of PP (>5 mg C m^{-3} h^{-1}) in the top 20 m of the water column soon after the initiation of deep water shoaling (Fig. 2b). The elevated PP

Table 1
Summary of hydrographic data for the CARIACO station

Day (Nov 1, 95 = day 1)	Date of cast	$T_{0-25\,m}$ (°C)	$PP_{0-100\,m}$ (g C m^{-2} d^{-1})
376	10-Nov-96	25.4	1.769
406	09-Dec-96	26.3	0.631
434	07-Jan-97	23.7	4.701
471	13-Feb-97	23.5	1.645
498	12-Mar-97	21.5	1.554
532	15-Apr-97	22.6	2.795
557	10-May-97	23.2	2.493
595	17-Jun-97	24.6	1.038
616	08-Jul-97	23.3	0.794
624	16-Jul-97	22.6	n.m.
656	17-Aug-97	23.0	0.955
687	17-Sep-97	27.3	0.457
714	14-Oct-97	27.3	0.774
Nov 96–Oct 97 average		24.3	1.634
744	13-Nov-97	26.2	0.653
778	17-Dec-97	23.8	1.401
806	14-Jan-98	24.3	1.370
834	11-Feb-98	25.2	0.519
863	12-Mar-98	22.2	3.308
903	21-Apr-98	25.0	0.335
952	09-Jun-98	25.0	1.392
982	09-Jul-98	23.9	0.458
1009	05-Aug-98	27.4	0.589
1036	01-Sep-98	27.2	0.570
1079	14-Oct-98	26.2	1.147
Nov 97–Oct 98 average		25.1	1.067
1106	10-Nov-98	27.0	0.611
1142	16-Dec-98	26.8	0.727
1169	12-Jan-99	24.1	1.818
1198	10-Feb-99	22.3	4.291
1220	04-Mar-99	23.6	1.274
1254	07-Apr-99	25.4	0.441
1283	06-May-99	25.1	1.283
1315	08-Jun-99	25.0	2.019
1353	15-Jul-99	25.2	1.246
1380	11-Aug-99	25.5	1.034
1414	14-Sep-99	28.0	0.605
1435	05-Oct-99	27.7	0.448
Nov 98–Oct 99 average		25.5	1.316

Note: $T_{0-25\,m}$, average temperature for the upper 25 m of the water column estimated from the hydrocast data presented in Fig. 2; $PP_{0-100\,m}$, cumulative primary productivity estimated for the upper 100 m of the water column based on the data presented in Fig. 2; n.m., not measured.

rates (>2 mg C m^{-3} h^{-1}) in the surface ocean extended for a long period all the way to August of 1997.

The second and third years of the study showed significant contrasts to the first one. For example, during the second year, the peak in surface PP was temporarily interrupted by the stratification that developed between December 1997 and February 1998 (Fig. 2b). The low rates (<2 mg C m^{-3} h^{-1}) measured in the top 20 m of the water column during February 1998 were a result of this event. It is interesting to note that this upwelling event was characterized by a relatively shallow high productivity zone early in the cycle, a sharp decrease in surface productivity in April, and the development of a sub-surface productivity maximum in May following the onset of thermal stratification (Fig. 2b). The main upwelling event in the third year of the study was relatively weak (Fig. 2a). However, unlike the 1997–1998 cycle, it was not disrupted by stratification and yielded relatively high PP rates (>2 mg C m^{-3} h^{-1}) over the top 20 m from December 1998 until March 1999 (Fig. 2b). It is also important to note that a sub-surface PP maximum (0.5 mg C m^{-3} h^{-1}) was evident early on in this upwelling cycle (December 1998), a feature that was not observed in either of the two previous years (Fig. 2b).

The secondary upwelling events in all three cycles also produced relatively elevated PP rates that exceeded 1 mg C m^{-3} h^{-1} in the summer months of the 3 years (Fig. 2b). Most interestingly, although the cooling of the water column was least intense during the third year (Fig. 2a), there was a prolonged period of relatively high productivity (2 mg C m^{-3} h^{-1}) from May to August of 1999 that extended down to 40 m (Fig. 2b).

In order to summarize the trends in PP, we chose to calculate the depth-integrated rates of cumulative PP over the top 100 m of the water column ($PP_{0-100\,m}$ in units of g C m^{-2} d^{-1}) for each month (Table 1). Using these cumulative monthly data, we were able to estimate annual $PP_{0-100\,m}$ averages for three upwelling-stratification cycles of this study. The 1996–1997 annual period was the most productive with average daily PP rates of 1.6 g C m^{-2} d^{-1}. Somewhat surprisingly, given its relatively high annual average surface temperature, the 1998–1999 cycle displayed the second highest average daily PP values (1.3 g C m^{-2} d^{-1}), a result of the high amount of

PP that occurred below 20 m in this year. The 1997–1998 period, which coincided with El Niño conditions, was the least productive (1.1 g $C\,m^{-2}\,d^{-1}$) of the three upwelling cycles examined in this study.

4.3. Sediment trap particle compositions

We observed significant seasonal differences in the compositions of the materials settling through the water column of the Cariaco Basin (Table 2). For example, the %OC of sediment trap samples typically reached high values of >10% during upwelling periods (December–March) in all three annual cycles. In contrast, periods of high stratification (June–October) were characterized by settling materials with relatively low %OC of 4–8% (Table 2). A similar pattern was observed for the %Opal of sediment trap samples, with high values (15–40%) typically measured during upwelling periods and low opal content during periods of water column stratification (%Opal <10%). On the other hand, the $\%CaCO_3$ of settling materials showed much less pronounced seasonal variability in all 3 years of the study. In general, sediment trap samples from both upwelling and stratification periods were characterized by $CaCO_3$ contents of 10–15%. Unlike OC and Opal, there were significant decreases in the $\%CaCO_3$ of the deeper trap (B and C) samples relative to those obtained from trap A. Finally, the ΣAlk_{37} contents of sediment traps failed to show any notable seasonal trend and generally ranged from 10 to 50 μg/g sample. Notably, unlike any of the other elements quantified, the deeper traps consistently displayed higher ΣAlk_{37} concentrations than their shallower counterparts.

The seasonal trends in the composition of sinking particles are evident in the elemental ratios of sediment trap samples (Fig. 3). For example, biogenic silica to OC weight ratios (Si/OC), which ranged from 0.2 to 1.2 in all three traps, were highest during the periods of strong upwelling and high PP, whereas they decreased during periods of stratification and low productivity (Fig. 2). This trend was most obvious during the 1996–1997 upwelling cycle when high Si/OC ratios (>0.5) were detected in all three traps from November 1996 to June 1997 (Fig. 3). In contrast, the two other upwelling cycles were characterized by much shorter periods of high Si/OC ratios, especially during the 1997–1998 period when ratios >0.5 were measured only in November and December. The seasonal trends in Si/OC ratios most likely reflect the contributions from diatoms to the settling materials in Cariaco Basin, which appeared to be directly related to upwelling and PP. There were no clear trends in the Si/OC ratios with depth, indicating organic matter and opal behave similarly during their vertical transport.

In contrast to the Si/OC ratios, the inorganic carbon to organic carbon weight ratios (IC/OC) generally displayed the highest values (>0.2) during periods of strong stratification and low productivity, whereas low values (<0.1) were generally observed in settling particles following periods of upwelling and high PP. This trend was most obvious during the 1996–1997 upwelling cycle, when IC/OC ratios reached values ⩽0.05 in all three traps from February to April 1997 (Fig. 3), periods of intense upwelling and PP (Fig. 2). IC/OC ratios increased later that year, reaching values >0.2 from August to November, during which high stratification led to very low levels of PP (Fig. 2). In general, the same relationship between upwelling/production and IC/OC ratios was observed in the other two upwelling cycles although the trends were less clear because of the changes in hydrography. For example, during the 1997–1998 cycle, upwelling was cut short by the stratification of the upper water column between late March and early June (Fig. 2). This period of low productivity coincided with an increase in the IC/OC ratios of settling particles collected in trap A. IC/OC ratios in trap A decreased during the secondary upwelling event in late June–July 1998 and then increased during the strong stratification that developed between August and December of that year. IC/OC ratios in traps B and C generally followed the trends measured in trap A, although there were several instances (e.g., September–October 1997; March–April 1998; March–April 1999) when the deeper traps recorded significantly lower ratios.

The C_{37} alkenones to OC weight ratios (ΣAlk_{37}/OC) in sinking materials from all traps ranged

Table 2
Compositions of sediment trap samples from the CARIACO station

Deployment code	Cup open	Cup close	Mid-day (11-1-95 = 1)	Duration (days)	Total Mass Flux ($g m^{-2} d^{-1}$)			%OC (g/100 g)			%Opal (g/100 g)			%$CaCO_3$ (g/100 g)			ΣAlk_{37} (μg/g)		
					Trap A (275 m)	Trap B (455 m)	Trap C (930 m)	Trap A (275 m)	Trap B (455 m)	Trap C (930 m)	Trap A (275 m)	Trap B (455 m)	Trap C (930 m)	Trap A (275 m)	Trap B (455 m)	Trap C (930 m)	Trap A (275 m)	Trap B (455 m)	Trap C (930 m)
car3-01	11/08/96	11/22/96	381	14	0.509	0.357	0.246	7.8	8.6	9.5	17.7	18.8	17.7	12.0	11.5	10.6	35.2	20.0	25.3
car3-02	11/22/96	12/06/96	395	14	1.521	1.706	1.380	5.3	5.1	5.6	8.8	9.0	7.8	9.3	8.3	8.6	—	—	—
car3-03	12/06/96	12/20/96	409	14	0.346	0.225	0.207	7.3	7.7	8.2	9.8	9.0	10.5	8.9	10.7	8.0	13.4	11.5	12.0
car3-04	12/20/96	01/03/97	423	14	0.408	0.262	0.202	10.0	10.5	11.4	19.2	19.0	20.3	15.6	13.4	14.3	—	—	—
car3-05	01/03/97	01/17/97	437	14	0.403	0.379	0.307	11.3	10.1	11.9	25.9	22.5	23.8	10.9	11.1	13.7	53.6	50.9	47.7
car3-06	01/17/97	01/31/97	451	14	0.267	0.133	0.240	13.0	13.7	14.0	18.2	15.4	16.3	6.7	7.8	12.1	—	—	—
car3-07	01/31/97	02/14/97	465	14	0.234	0.129	0.102	12.9	14.5	14.1	20.1	20.9	19.6	7.7	6.7	8.0	19.6	13.7	—
car3-08	02/14/97	02/28/97	479	14	0.779	0.384	0.276	11.4	12.1	13.6	26.9	28.2	30.2	5.4	5.5	3.5	—	—	19.5
car3-09	02/28/97	03/14/97	493	14	0.757	0.498	0.284	12.5	13.4	15.0	30.8	30.2	36.7	5.7	4.2	3.1	14.1	14.4	—
car3-10	03/14/97	03/28/97	507	14	0.875	0.453	0.712	14.1	14.2	17.7	30.2	27.6	29.7	4.0	4.1	3.1	—	—	15.5
car3-11	03/28/97	04/11/97	521	14	n.r.	n.r.	0.186	n.r.	n.r.	15.3	n.r.	n.r.	24.4	n.r.	n.r.	3.3	n.r.	n.r.	—
car3-12	04/11/97	04/25/97	535	14	n.r.	n.r.	0.218	n.r.	n.r.	15.0	n.r.	n.r.	19.0	n.r.	n.r.	1.7	n.r.	n.r.	—
car3-13	04/25/97	05/15/97	546	11	n.r.	n.r.	0.059	n.r.	n.r.	11.8	n.r.	n.r.	13.0	n.r.	n.r.	3.7	n.r.	n.r.	—
car4-01	05/15/97	05/22/97	562	7	1.030	0.632	0.642	11.5	11.3	10.0	23.5	25.7	18.0	12.3	9.2	8.9	9.0	14.2	17.3
car4-02	05/22/97	06/05/97	576	14	2.047	1.240	1.043	8.8	7.9	9.4	15.5	19.8	19.1	11.5	9.5	10.9	—	—	—
car4-03	06/05/97	06/19/97	590	14	1.056	0.149	0.189	7.7	6.3	8.4	9.2	10.2	11.9	12.7	10.9	14.3	28.1	15.0	26.9
car4-04	06/19/97	07/03/97	604	14	0.409	0.086	0.068	11.5	7.0	9.5	5.2	5.5	5.2	14.1	11.1	10.4	—	—	—
car4-05	07/03/97	07/17/97	618	14	0.965	0.167	0.168	7.5	13.2	11.8	11.0	17.5	14.5	9.1	7.4	10.2	10.6	23.3	23.5
car4-06	07/17/97	07/31/97	632	14	0.661	0.064	0.071	7.6	17.4	16.7	10.9	16.3	14.9	11.3	7.0	8.6	—	—	—
car4-07	07/31/97	08/14/97	646	14	1.137	0.482	0.162	7.5	8.8	12.6	7.4	9.8	10.1	11.5	8.3	9.8	12.7	40.6	97.8
car4-08	08/14/97	08/28/97	660	14	0.422	0.047	0.034	6.7	9.8	10.0	7.3	7.4	—	11.7	11.5	20.9	—	—	—
car4-09	08/28/97	09/11/97	674	14	0.563	0.119	0.070	7.4	10.8	14.5	7.0	10.2	9.2	11.9	11.3	13.3	16.8	78.5	—
car4-10	09/11/97	09/25/97	688	14	0.756	0.135	0.059	5.9	7.5	8.9	6.0	7.6	8.2	12.5	10.5	12.8	—	—	—
car4-11	09/25/97	10/09/97	702	14	0.602	0.079	0.022	5.8	7.4	9.7	3.7	5.9	—	13.1	12.6	12.0	29.1	7.3	—
car4-12	10/09/97	10/23/97	716	14	0.381	0.361	0.050	5.6	7.1	7.3	4.9	4.6	5.0	14.6	4.0	11.9	—	—	—
car4-13	10/23/97	11/13/97	727	11	0.480	0.085	0.047	4.5	6.7	8.3	4.6	3.8	—	13.9	9.0	7.9	1.3	—	—
Nov 96–Oct 97 average					0.722	0.355	0.271	8.8	10.1	11.5	14.1	15.0	16.7	10.7	8.9	9.4	20.3	26.3	23.8
car5-01	11/13/97	11/20/97	744	7	0.735	0.565	0.371	9.5	6.8	6.9	18.1	16.4	13.0	21.0	23.4	22.8	8.5	11.3	11.7
car5-02	11/20/97	12/04/97	758	14	1.378	0.683	0.489	7.4	7.6	8.5	11.4	14.3	15.5	11.9	13.3	13.8	—	—	—
car5-03	12/04/97	12/18/97	772	14	1.013	1.019	0.731	11.0	9.0	8.7	21.0	22.0	21.6	8.5	7.8	5.5	24.7	37.2	32.4
car5-04	12/18/97	01/01/98	786	14	1.017	1.327	0.515	6.0	5.5	5.8	8.6	8.6	8.8	8.1	7.5	6.6	—	—	—
car5-05	01/01/98	01/15/98	800	14	0.582	0.671	0.558	11.8	11.3	10.4	14.3	16.0	13.1	9.8	9.8	7.5	13.8	25.0	44.1
car5-06	01/15/98	01/29/98	814	14	0.078	0.259	0.224	12.3	7.6	8.0	8.1	7.5	7.8	11.6	12.1	12.8	—	—	—
car5-07	01/29/98	02/12/98	828	14	0.187	0.505	0.279	14.3	13.7	13.6	12.9	16.8	13.8	9.8	8.2	8.9	24.9	80.9	98.4
car5-08	02/12/98	02/26/98	842	14	0.266	0.185	0.105	7.0	8.8	9.9	6.6	7.0	6.7	14.3	11.1	10.7	—	—	—
car5-09	02/26/98	03/12/98	856	14	0.805	0.139	0.109	6.2	11.8	12.0	8.2	16.1	12.5	14.9	6.8	9.9	7.2	—	91.5
car5-10	03/12/98	03/26/98	870	14	2.479	0.397	0.339	7.1	17.6	17.1	9.6	22.4	21.5	13.0	2.9	2.7	—	—	—
car5-11	03/26/98	04/09/98	884	14	1.537	0.435	0.451	9.4	17.2	17.0	10.0	11.9	10.5	12.9	2.4	0.8	10.7	64.9	—

car5-12	04/09/98	04/23/98	898	14	0.877	0.210	0.234	7.7	11.7	11.8	8.3	9.4	9.9	14.6	1.2	0.1	—	—	—
car5-13	04/23/98	05/03/98	909	11	0.628	0.157	0.108	7.2	11.2	13.9	7.3	9.4	8.2	16.1	0.7	5.5	8.4	—	—
car6-01	06/03/98	06/10/98	946	7	0.672	0.286	0.255	9.6	9.9	9.8	8.9	7.8	6.3	17.9	15.9	18.8	32.7	31.6	36.5
car6-02	06/10/98	06/17/98	953	7	1.967	1.302	0.866	5.0	5.1	5.7	5.8	6.8	6.6	11.9	11.7	12.8	—	—	—
car6-03	06/17/98	06/24/98	960	7	1.072	0.643	0.574	7.7	8.1	8.7	5.6	5.3	5.1	14.5	11.6	11.0	30.7	21.3	28.2
car6-04	06/24/98	07/01/98	967	7	0.495	0.453	0.312	11.2	11.1	12.9	7.9	7.9	7.4	14.3	12.2	11.2	—	—	—
car6-05	07/01/98	07/15/98	981	14	0.489	0.279	0.181	11.6	9.9	11.7	11.3	11.5	11.1	11.0	9.5	9.1	32.3	31.2	43.6
car6-06	07/15/98	07/29/98	995	14	0.469	0.591	0.333	17.3	12.8	15.3	17.6	15.5	16.2	7.0	7.1	6.5	25.2	32.0	—
car6-07	07/29/98	08/12/98	1009	14	0.661	0.473	0.215	6.6	6.1	9.0	7.6	7.6	8.2	8.8	8.4	7.3	13.9	17.1	32.9
car6-08	08/12/98	08/26/98	1023	14	0.601	0.041	0.033	6.8	15.9	14.7	8.2	7.7	8.7	12.4	11.2	12.2	—	—	—
car6-09	08/26/98	09/09/98	1037	14	1.131	0.497	0.297	5.7	6.6	7.5	6.7	6.7	6.0	9.7	8.1	7.0	17.0	13.8	30.4
car6-10	09/09/98	09/23/98	1051	14	0.938	0.378	0.185	6.0	7.8	9.9	8.9	12.6	16.3	10.0	8.9	8.7	—	—	—
car6-11	09/23/98	10/07/98	1065	14	1.048	0.295	0.154	7.8	12.7	15.8	11.3	16.9	17.3	11.4	10.8	10.2	41.7	27.6	31.2
car6-12	10/07/98	10/21/98	1079	14	0.689	0.174	0.077	6.2	7.7	10.3	9.1	11.3	11.9	14.5	12.7	12.2	—	—	—
car6-13	10/21/98	11/02/98	1091	12	0.559	0.041	0.021	5.5	6.4	—	8.1	9.9	—	16.0	12.5	—	10.8	—	—
Nov 97–Oct 98 average					0.860	0.462	0.308	8.6	10.0	11.0	10.1	11.7	11.4	12.5	9.5	9.4	20.2	32.8	40.1
car7-01	11/07/98	11/19/98	1110	14	0.690	0.404	0.445	8.0	6.9	6.5	8.4	8.4	7.9	15.7	16.6	13.3	5.4	16.3	22.9
car7-02	11/21/98	12/03/98	1124	14	0.902	0.477	0.361	7.5	7.5	7.2	14.1	16.4	14.7	17.3	15.1	13.0	37.9	43.4	—
car7-03	12/05/98	12/17/98	1138	14	0.735	0.677	0.557	6.3	6.4	6.8	7.8	8.6	8.8	14.1	14.3	13.3	16.8	32.9	43.4
car7-04	12/19/98	12/31/98	1152	14	0.255	0.158	0.111	9.0	9.5	11.7	11.4	15.8	14.4	13.3	8.9	10.8	—	—	—
car7-05	01/02/99	01/14/99	1166	14	0.143	0.135	0.111	12.6	12.6	10.8	19.6	20.7	18.0	16.1	14.8	17.1	—	—	73.6
car7-06	01/16/99	01/28/99	1180	14	0.145	0.198	0.153	13.8	14.6	15.7	12.4	15.2	16.3	20.0	16.7	19.6	—	—	—
car7-07	01/30/99	02/11/99	1194	14	0.225	0.501	0.378	14.7	12.0	18.8	17.3	17.4	20.6	16.0	14.0	10.3	—	40.6	23.0
car7-08	02/13/99	02/25/99	1208	14	0.065	0.186	0.142	21.5	15.6	16.9	13.8	15.1	14.8	7.7	14.5	14.1	—	—	—
car7-09	02/27/99	03/11/99	1222	14	0.078	0.183	0.138	11.5	13.7	15.9	10.3	8.2	8.0	16.7	13.7	13.0	—	—	140.4
car7-10	03/13/99	03/25/99	1236	14	0.136	0.227	0.101	13.2	11.9	14.9	8.8	12.3	11.9	28.7	13.7	11.9	—	—	—
car7-11	03/27/99	04/08/99	1250	14	0.379	0.554	0.270	9.8	11.4	11.1	11.6	16.6	16.7	16.4	4.7	6.7	32.7	60.3	105.3
car7-12	04/10/99	04/22/99	1264	14	0.538	0.269	0.145	8.7	10.0	11.7	9.9	12.6	13.1	15.6	4.8	2.1	24.5	23.1	—
car7-13	04/24/99	05/06/99	1273	9	0.444	0.821	0.123	8.1	7.1	—	9.7	9.3	9.8	11.7	15.2	11.4	—	—	—
car8-01	05/06/99	05/18/99	1290	14	2.413	1.935	1.669	5.4	4.6	4.9	6.8	7.4	7.0	9.0	9.7	10.0	—	—	7.4
car8-02	05/20/99	06/01/99	1304	14	0.744	0.440	0.497	10.6	8.6	7.2	8.1	8.0	7.4	16.3	13.9	12.7	44.0	26.4	—
car8-03	06/03/99	06/15/99	1318	14	0.541	0.583	0.565	12.9	10.5	9.7	12.9	14.4	11.5	12.2	8.9	11.2	—	—	46.1
car8-04	06/17/99	06/29/99	1332	14	0.921	0.889	0.454	10.9	10.0	12.1	9.4	8.8	9.7	11.7	10.8	10.4	68.0	78.4	—
car8-05	07/01/99	07/13/99	1346	14	0.622	0.287	0.159	9.8	10.5	13.2	8.0	10.5	8.8	12.7	13.2	13.2	—	—	50.3
car8-06	07/15/99	07/27/99	1360	14	0.730	0.162	0.143	8.8	15.4	14.7	8.4	12.3	9.8	12.6	11.1	24.5	—	—	—
car8-07	07/29/99	08/10/99	1374	14	0.429	0.224	0.234	11.0	12.9	11.5	10.0	14.7	12.4	11.9	10.7	11.1	—	50.0	45.7
car8-08	08/12/99	08/24/99	1388	14	0.483	0.147	0.309	8.7	8.2	8.4	6.6	7.5	7.4	13.0	9.5	12.6	28.6	19.2	—
car8-09	08/26/99	09/07/99	1402	14	0.753	0.137	0.167	6.6	7.3	6.6	5.8	5.8	6.0	11.2	7.3	10.8	—	—	—
car8-10	09/09/99	09/21/99	1416	14	0.887	0.155	0.120	6.1	8.4	9.2	5.2	6.5	5.8	9.6	11.0	10.0	18.3	—	—
car8-11	09/23/99	10/05/99	1430	14	1.199	0.201	0.203	5.6	7.0	8.4	5.1	5.5	5.4	10.4	8.0	7.9	—	—	—
car8-12	10/07/99	10/19/99	1444	14	1.213	0.110	0.097	5.4	6.4	6.2	4.9	5.5	6.2	9.5	10.0	10.3	12.1	—	—
car8-13	10/21/99	11/02/99	1456	12	1.285	0.133	0.097	5.1	9.0	11.3	4.7	6.0	5.2	10.8	9.0	8.2	—	—	—
Nov 98–Oct 99 average					0.652	0.392	0.298	9.7	9.9	10.9	9.7	11.1	10.7	13.9	11.5	11.9	28.8	39.1	55.8

Note: Dates on which sediment trap cups were opened and closed are indicated; %OC, weight percent organic carbon content; %Opal, weight percent biogenic opal content; %$CaCO_3$, weight percent calcite content; ΣAlk_{37}, concentration of C_{37} methyl alkenones in sediment trap materials (micrograms/gram); —, not determined; n.r., sediment trap samples not recovered because of clogging of the sediment trap.

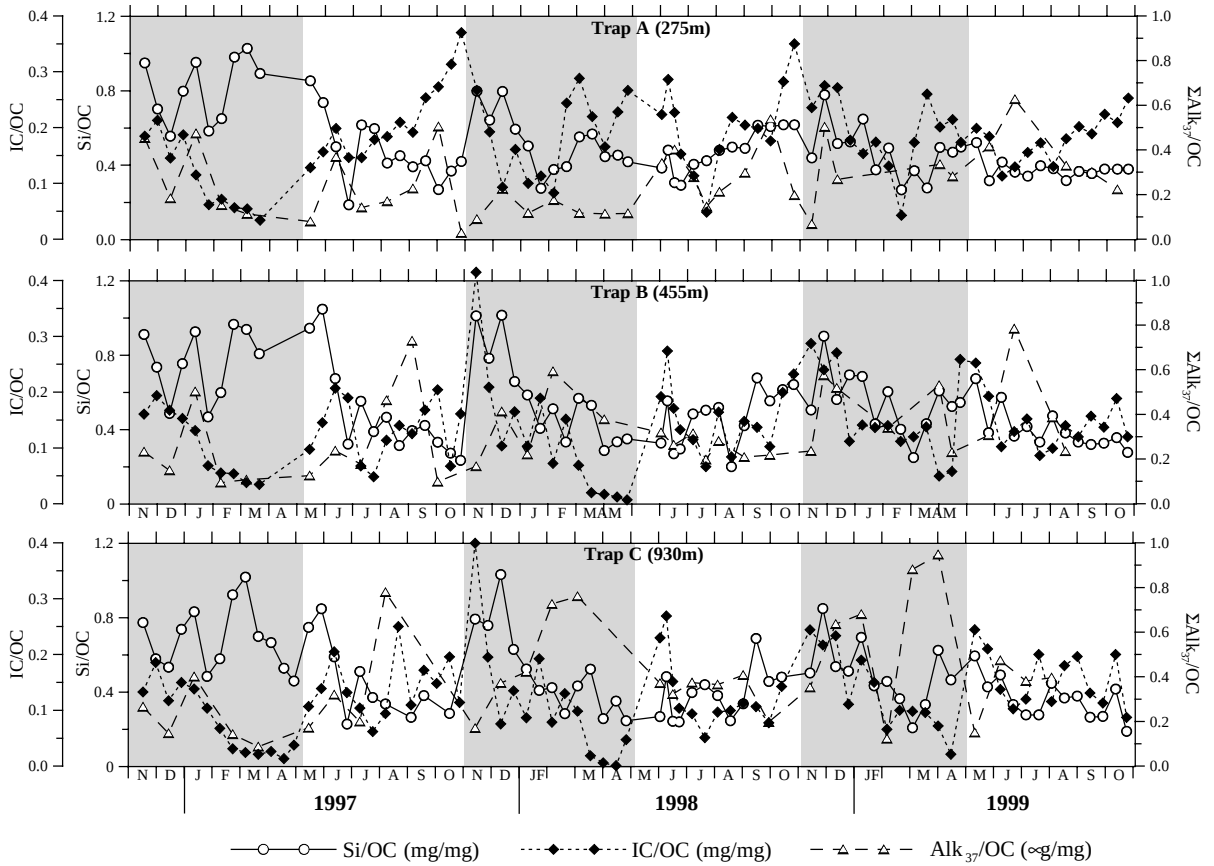

Fig. 3. Biogenic ratios of sinking materials collected from traps A, B, and C at the Cariaco station. Weight ratios of biogenic silica to organic carbon (Si/OC), inorganic carbon to organic carbon (IC/OC) and sum of C_{37} alkenones to organic carbon ($\Sigma Alk_{37}/OC$) are plotted for each of the sediment trap samples over the study period. The alternating shaded areas in each graph indicate the duration of each 6-month trap deployment.

from 0.1 to 0.8 μg/mg and displayed marked seasonal and depth variability. In some cases, such as the 1996–1997 upwelling cycle, the distributions of $\Sigma Alk_{37}/OC$ ratios were similar to those of IC/OC ratios with low values ($\leqslant 0.2$) measured from February to May 1997 (high productivity periods) and high values (0.2–0.8) during the low productivity season from June to early October 1997 (Fig. 3). However, this relationship between IC/OC and $\Sigma Alk_{37}/OC$ ratios breaks down in several instances of the trap study. For example, low $\Sigma Alk_{37}/OC$ ratios are measured in trap A during October–November 1997, March–April 1998, and November 1998, all of which are periods of high IC/OC ratios. Most likely, the decoupling between IC/OC and $\Sigma Alk_{37}/OC$ ratios in these samples reflects changes in the contribution of alkenone producers to the total $CaCO_3$ export. High $\Sigma Alk_{37}/OC$ ratios (>0.4) that were significantly higher than those measured in trap A samples were obtained in traps B and C during August–September 1997, February–March 1998, and February–March 1999 periods. These data indicate that C_{37} alkenones are less sensitive to diagenetic losses during vertical transport through the Cariaco Basin water column than bulk OC.

4.4. Sediment core compositions

The AMS ^{14}C dates of monospecific samples of the planktic foraminifer *G. bulloides* isolated from

19 sedimentary horizons are presented in Table 3. AMS dates were converted to calendar years according to Stuiver and Braziunas (1993) and a reservoir correction of 420 years (Hughen et al., 1998; Black et al., 1999). The ages, accumulation rates, and biogenic compositions of the sedimentary horizons sampled from the gravity core are presented in Table 4. Sediment accumulation rates were calculated from the interpolated ages and the dry bulk densities determined for each horizon (Black et al., 2001). The ^{14}C ages indicated that the gravity core represents almost 5500 years of sedimentation and that the last 300 years of accumulation were lost from the top of the core during sampling. Throughout most of the core, the calculated accumulation rates ranged from 0.02 to 0.04 $g\,cm^{-2}\,yr^{-1}$. The major exceptions to this trend were observed in the top 20 cm of the gravity core, with very low rates ($<0.01\,g\,cm^{-2}\,yr^{-1}$) estimated for the top 10 cm but extremely high values ($0.18\,g\,cm^{-2}\,yr^{-1}$) for the 15–15.5 cm horizon. At this point, it is unclear if these "unusual" accumulation rate values are due to artifacts related to disturbance associated with coring. Hence, we did not use these samples for biogenic burial flux calculations (see Section 5).

Table 3
Results of AMS radiocarbon dating of Cariaco Basin gravity core CAR7-2 at the center for AMS (CAMS), Lawrence Livermore National Laboratory

Core depth (cm)	CAMS no.	Meas. age[a] (^{14}C yr BP)	Cal. age[b] (cal. yr BP)	Cal. age range $\pm 1\sigma$
0.5	62,947	540±40	195	156–294
5.2	62,948	680±40	345	324–376
10.2	62,949	950±50	578	553–607
15.2	62,950	1180±40	750	718–786
20.2	62,951	1210±30	777	750–809
25.2	62,952	1260±50	828	780–914
30.2	62,953	1290±40	875	818–936
35.2	62,954	1400±40	978	970–1008
40.2	62,955	1460±40	1027	992–1084
45.2	62,956	1520±40	1102	1050–1146
50.2	62,957	1640±40	1237	1199–1287
55.2	62,958	1780±40	1349	1326–1383
60.2	62,959	1850±40	1417	1374–1457
65.2	62,960	1870±40	1438	1393–1486
100.2	62,961	2520±40	2198	2163–2291
130.2	62,962	3020±40	2810	2738–2846
160.2	62,963	3580±40	3500	3541–3530
190.2	62,964	4250±50	4402	4322–4454
220.2	62,965	5070±40	5483	5379–5508

Note: Meas. age, measured age; cal. age, calendar age; yr BP, years before present.

[a] Radiocarbon dates listed here have not been corrected for the 420-year age of the Cariaco Basin surface ocean reservoir.

[b] ^{14}C ages were converted to calendar years according to Stuiver and Braziunas (1993) and Black et al. (1999).

Weight percent OC ranged from 4% to 5.5% and showed a general down core decrease over the top 180 cm (Table 4). Similarly, opal, which ranged from 3% to 5%, also showed an overall decrease with depth (Table 4). In contrast, $\%CaCO_3$ increased from 17% (5.5 cm depth) to 25% midway through the core (120 cm). Below this depth, $\%CaCO_3$ remained relatively constant ranging from 20% to 24%. The concentrations of ΣAlk_{37} decreased steeply over the top 30 cm of the core from a value of 7 to ~2 μg/g. Between 30 and 80 cm, ΣAlk_{37} concentrations increased steadily to a maximum of 8 μg/g, followed by another steady decrease to values of ~2 μg/g measured at 140 cm below the core top. Moderately elevated values were measured below that depth, with ΣAlk_{37} concentrations exceeding 4 μg/g between 160 and 180 cm (Table 4).

The down core distribution of biogenic ratios (Fig. 4) revealed relatively constant Si/OC ratios that ranged from 0.4 to 0.5. The major exception was the low value (0.3) measured at 70 cm. Overall, the Si/OC ratios of sediment samples were considerably lower than those measured in sinking particles during upwelling periods (>0.5, Fig. 3) but comparable to the values obtained during the rest of the year. In contrast, IC/OC ratios steadily increased from values ~0.45 near the top of the core to values exceeding 0.65 in sediments from 150 to 200 cm depth. Lower IC/OC ratios (0.5–0.6) were measured in the deepest part of the core. Unlike the Si/OC data, the sediment IC/OC ratios measured throughout the gravity core (0.4–0.7) were consistently higher than those measured in the sinking particulates from the Cariaco Basin water column (0.1–0.4). Three peaks in ΣAlk_{37}/OC ratios (>0.1) are evident at the top of the core, between 70 and 90 cm and between 160 and 190 cm (Fig. 4). Minima in ΣAlk_{37}/OC ratios (~0.05) were observed in sediments from 25 cm and

Table 4
Gravity core (CAR 7-2) sediment data

Horizon depth (cm)		Cal. age (yr BP)	Sed. rate ($g\,cm^{-2}\,yr^{-1}$)	%OC (g/100 g sed)	%Opal (g/100 g sed)	$\%CaCO_3$ (g/100 g sed)	ΣAlk_{37} (μg/g sed)
Top	Bottom						
1.0	1.5	300	0.007	4.98	4.79	21.4	7.14
5.0	5.5	457	0.005	4.97	n.d.	17.5	4.05
10.0	10.5	678	0.007	5.14	5.11	18.0	3.57
15.0	15.5	761	0.167	5.32	4.39	20.5	4.34
19.0	19.5	776	0.047	4.95	5.01	18.9	4.17
25.0	25.5	835	0.038	4.92	4.46	19.9	1.77
30.0	30.5	892	0.031	4.78	4.84	21.6	2.51
36.0	36.5	981	0.024	5.30	4.79	20.6	2.85
40.0	40.5	1046	0.024	5.37	4.83	18.2	3.47
45.0	45.5	1130	0.024	5.12	5.06	20.5	2.56
50.0	50.5	1217	0.024	5.32	4.85	21.7	4.28
59.0	59.5	1378	0.024	4.85	4.79	22.4	3.71
70.0	70.5	1598	0.021	5.18	3.08	20.7	6.68
78.0	78.5	1768	0.022	4.82	4.46	20.1	7.98
89.5	90.0	2000	0.024	5.25	5.19	21.4	6.06
100.0	100.5	2205	0.023	4.97	4.97	20.1	4.09
110.0	110.5	2408	1.023	4.63	4.09	22.5	3.87
120.0	120.5	2610	2.023	5.03	n.d.	25.3	2.98
130.0	130.5	2811	3.023	4.78	n.d.	22.2	3.35
140.0	140.5	3049	4.023	4.53	3.45	21.6	2.35
150.0	150.5	3286	5.023	4.35	4.00	24.3	3.66
160.0	160.5	3521	6.023	4.10	n.d.	23.1	5.25
170.0	170.5	3817	7.023	4.31	3.70	23.2	5.34
180.0	180.5	4112	8.023	4.07	2.96	23.3	4.53
190.0	190.5	4405	9.023	4.55	3.85	20.7	5.70
200.0	200.5	4771	10.023	4.59	4.16	22.1	4.19
210.0	210.5	5134	11.023	4.33	3.64	21.8	3.84
220.0	220.5	5494	12.023	4.31	4.50	20.7	3.48

Note: Cal. age (calendar age) and sed. rate (sediment accumulation rate) are based on age model by Black et al. (2001); %OC, weight percent organic carbon; %Opal, weight percent biogenic opal; $\%CaCO_3$, weight percent calcium carbonate; ΣAlk_{37}, total of C_{37} alkenone concentrations; n.d., not determined.

120–140 cm in the core. In contrast to Si/OC and IC/OC ratios, sediment ΣAlk_{37}/OC ratios (0.05–0.2) were always lower than the ΣAlk_{37}/OC ratios exhibited by sinking particles (0.2–0.8) throughout all periods.

5. Discussion

5.1. Seasonal trends in biogenic fluxes

Fluxes of OC, opal, $CaCO_3$ and ΣAlk_{37} settling through the water column in the Cariaco Basin (Fig. 5) were estimated by multiplying the contents of each sediment trap sample by the total material flux obtained during each collection interval (Table 2). The magnitude of the fluxes, especially those in trap A, varied significantly throughout each year, with the highest export rates for OC, opal, and $CaCO_3$ reaching peaks ($\geqslant 0.1\,g\,m^{-2}\,d^{-1}$) during periods of upwelling and high PP (Fig. 2). High export rates in trap A (Fig. 5) were also measured during the secondary upwelling events that characterized each annual cycle (i.e., July 97, June 98, May 99; Fig. 2). In contrast, low OC, opal, and $CaCO_3$ export rates ($\leqslant 0.1\,g\,m^{-2}\,d^{-1}$, Table 2) were measured during times of high water column stratification and low productivity such as

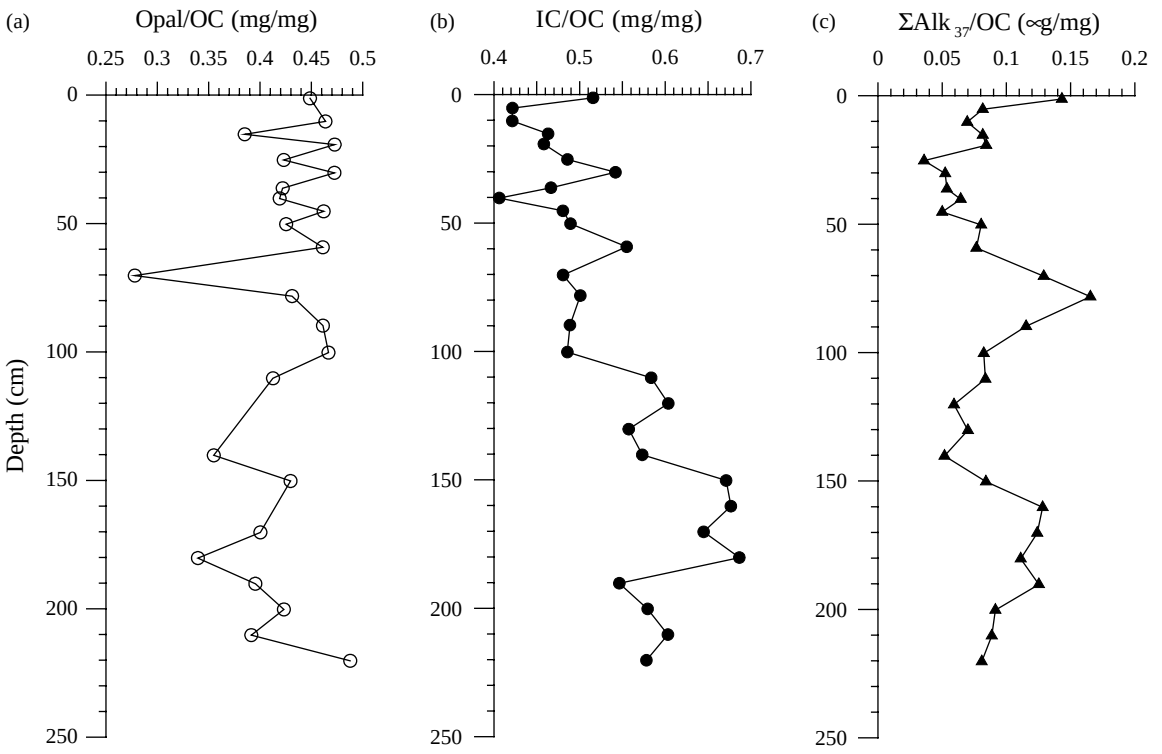

Fig. 4. Biogenic ratios of sediments from the gravity core (CAR7-2) in the Cariaco Basin. Weight ratios of (a) biogenic silica to organic carbon (Si/OC), (b) inorganic carbon to organic carbon (IC/OC) and (c) sum of C_{37} alkenones to organic carbon (ΣAlk_{37}/OC) are plotted for each of the sediment horizons analyzed.

August 97, July 98, and July/August 1999. The same cannot be said for ΣAlk_{37} fluxes, which showed much less pronounced seasonal variability with only secondary peaks in flux that coincided with upwelling events in July 1997 and June 1998. The larger ΣAlk_{37} flux events, during September 1998 and especially June 1999, occurred after high PP periods and significantly lagged the peaks in flux of the major biogenic constituents (Fig. 5).

Overall, the vertical fluxes of all four components measured in trap A (275 m water depth) were consistently higher than those observed in traps B (455 m) and C (930 m). These trends agree with our current understanding of how the vertical export of biogenic materials from the surface ocean is intensified with increased PP (e.g., Suess, 1980; Betzer et al., 1984; Pace et al., 1987) and is attenuated with depth by respiration and dissolution (e.g., Thunell et al., 2000 and references therein). However, there were several instances (e.g., November–December 1996, December 1997–February 1998, and January–March 1999) when the biogenic fluxes measured in the deeper traps were higher than those from shallower ones (Table 2, Fig. 5). The best way to illustrate these trends is to plot the flux efficiency (flux ratio × 100) between traps A and B and between traps B and C. Trap B flux efficiency estimates for TM (Fig. 6) exceed 100% during several months of 1998 and 1999, when fluxes in trap B exceeded those measured in trap A. Similar trends are obtained for OC, opal, $CaCO_3$ and ΣAlk_{37} flux efficiencies (data not shown).

Previous sediment trap studies have measured elevated fluxes in deeper traps and discussed the potential causes in detail, including inputs at depth, the effects of currents, and changes in the hydrodynamic properties of sinking particles (e.g.,

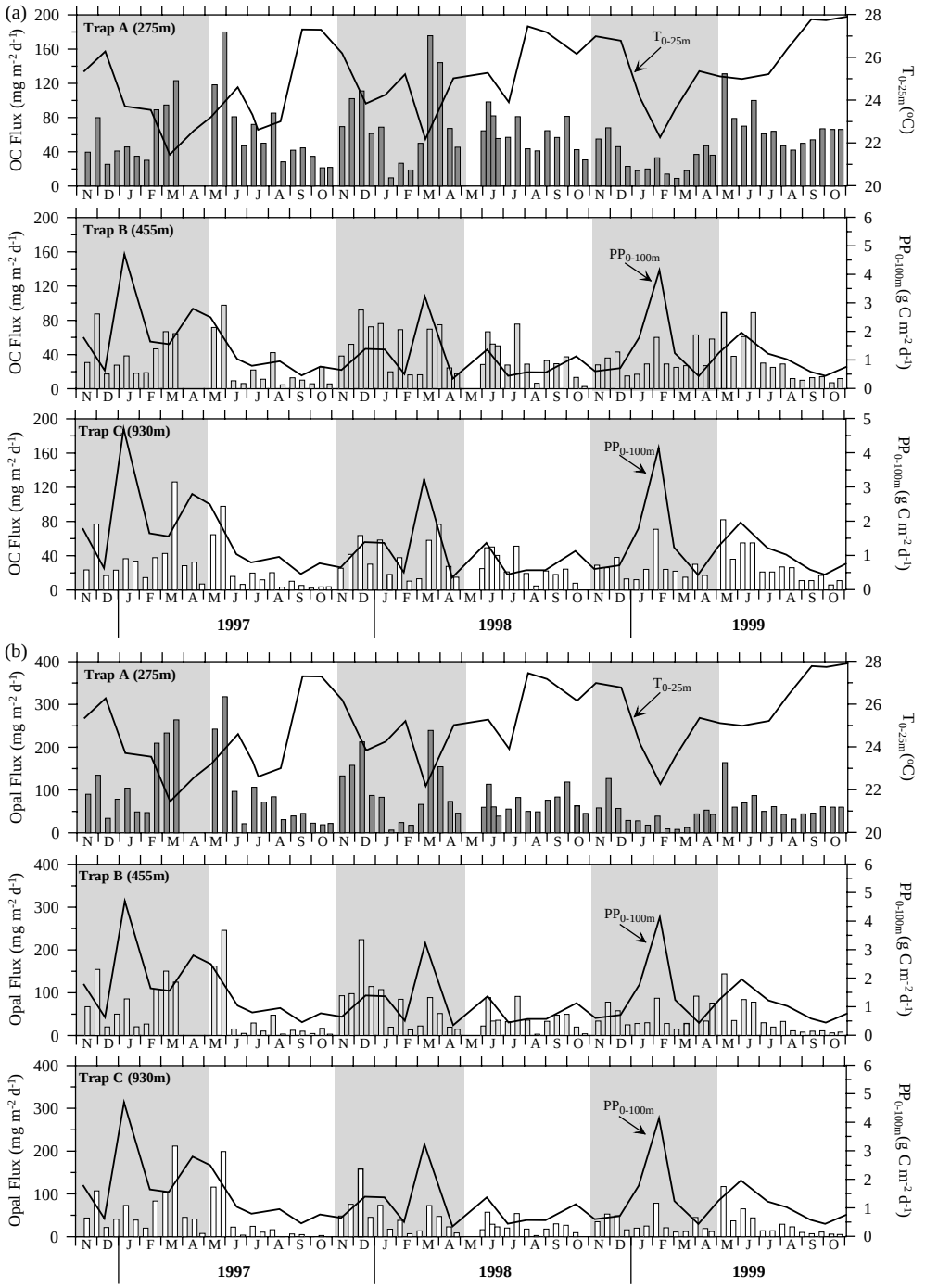

Fig. 5. Mean daily fluxes of (a) organic carbon, (b) biogenic opal, (c) $CaCO_3$, (d) long-chain C_{37} alkenones determined from the bi-weekly sediment trap deployments at the Cariaco station. All fluxes were calculated from the data in Tables 2 and 4. The alkenone fluxes were determined in fewer sediment trap samples because of limitations due to the amount of sample available. Included in these graphs are the records of average temperature in the top 0–25 m ($T_{0-25\,m}$) and average PP in the top 0–100 m of the water column ($PP_{0-100\,m}$) calculated from the monthly hydrocast data (Table 1). The alternating shaded areas in the graphs indicate the duration of each 6-month trap deployment during the study period.

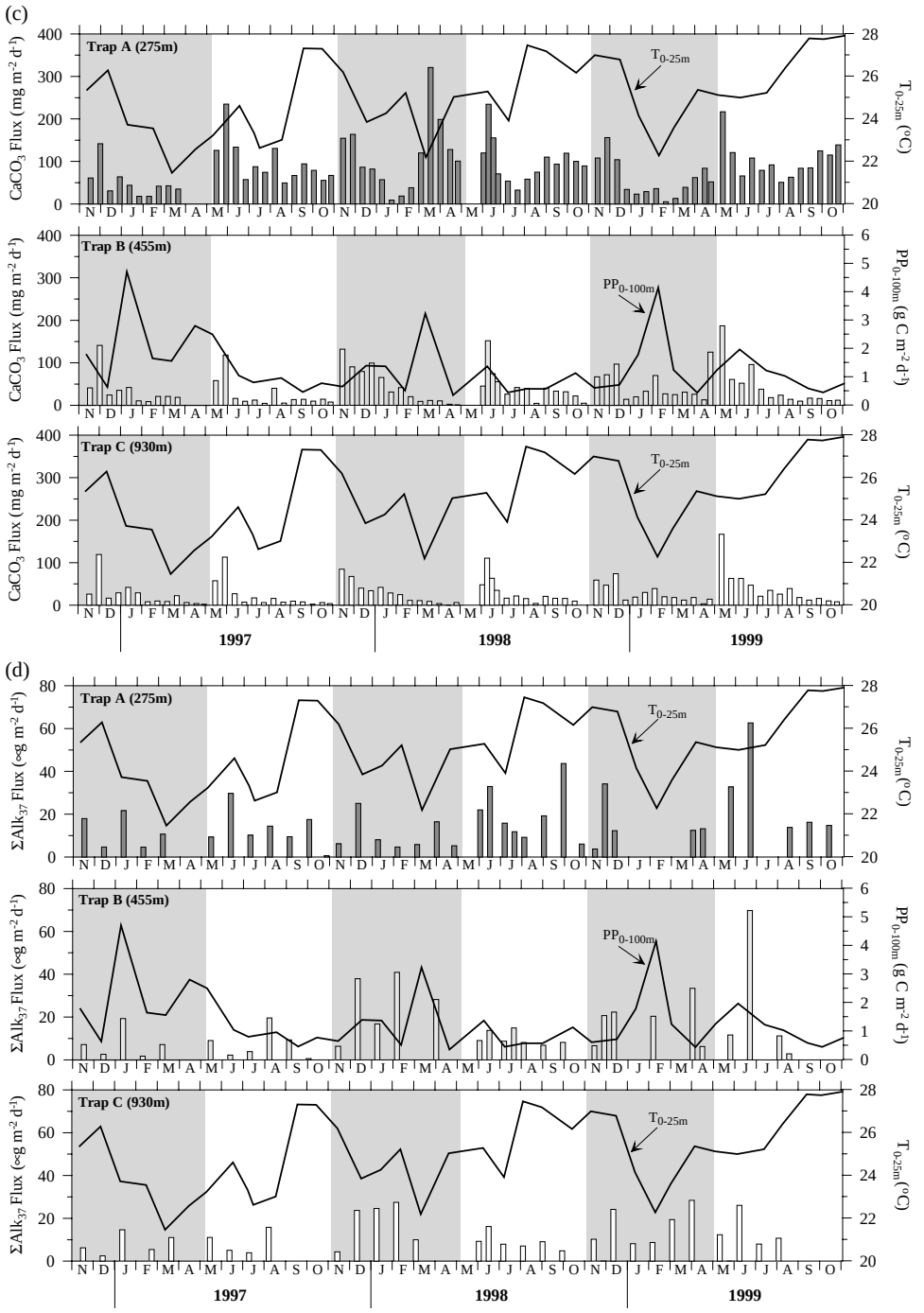

Fig. 5 (*continued*).

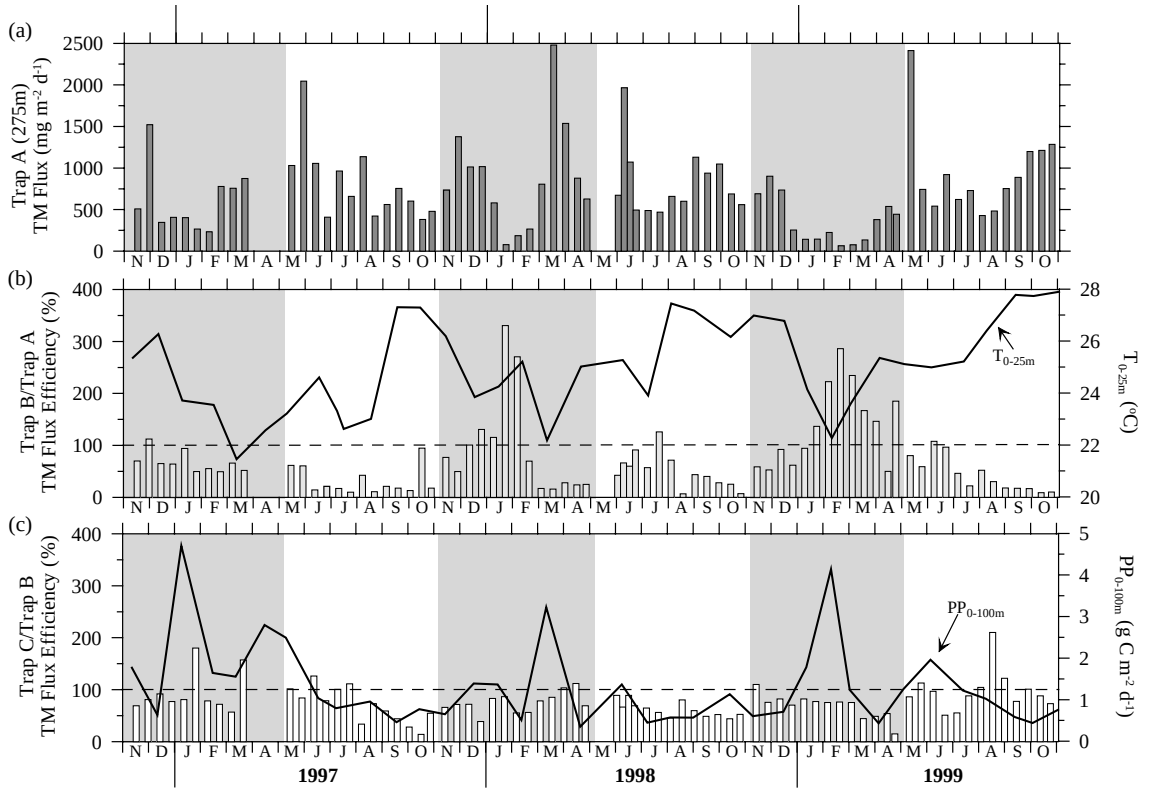

Fig. 6. (a) TM fluxes measured in trap A over the study period at the Cariaco station, (b) TM flux efficiencies between traps A and B, and (c) TM flux efficiencies between traps B and C. Flux efficiencies are defined as the ratio of the bottom trap over the top trap flux multiplied by 100. Flux efficiencies >100% indicate under-trapping by the top trap and/or additional inputs at depth to the bottom trap. See text for further discussion of these results. Included in these graphs are the records of average temperature in the top 0–25 m ($T_{0-25\,m}$) and average PP in the top 0–100 m of the water column ($PP_{0-100\,m}$) calculated from the monthly hydrocast data (Table 1). The alternating shaded areas in the graphs indicate the duration of each 6-month trap deployment during the study period.

Baker et al., 1988; Buesseler, 1991; Scholten et al., 2001; Yu et al., 2001). In our study, one likely explanation for some of the >100% trapping efficiency events is the partial clogging of the shallower traps during periods of high productivity (e.g., from January to March of 1999, Fig. 5). Indeed, the high PP rates between March and May of 1997 (Fig. 2) caused the complete clogging of several cups (Car3 11–13) from the two top traps during that period (Table 2). Other under-trapping events coincided with lateral sub-surface intrusions (Astor et al., 2003; Scranton et al., 2001) that propagate from the Caribbean Sea and episodically enter the Cariaco Basin (e.g., Andrade and Barton, 2000; Pauluhn and Chao, 1999). We speculate that the enhanced horizontal shear accompanying the intrusion events observed during December 1997–February 1998 (Astor et al., 2003; Scranton et al., 2001) might ultimately be responsible for the lower than expected fluxes recovered in the top trap during this period (Fig. 6). Finally, although bacterial activity appears to increase during sub-surface intrusions (Taylor et al., 2001), the addition of microbial-derived materials at depth cannot explain these trends since elevated fluxes of phytoplankton-derived materials such as opal, $CaCO_3$, and alkenones are measured in trap B.

As a separate issue, we note that $CaCO_3$ fluxes in the deeper traps (B and C) show an unusual trend unlike any of the other biogenic materials measured in this study. In these traps, $CaCO_3$

fluxes are consistently highest during the first or second sampling period of each 6-month deployment and then decrease with time (Fig. 5). Similar trends have been observed in other traps deployed in low oxygen water columns (Thunell, unpub. data). We suspect that post-collection IC precipitation may be occurring in the cups, perhaps facilitated by the anoxic conditions of the water column (e.g., Reimers et al., 1996; Sholkovitz, 1973). Although investigating this process is beyond the scope of this paper, these observations raise doubt on our the ability to use the vertical $CaCO_3$ water column fluxes obtained from the deeper traps to interpret the compositions measured in Cariaco Basin sediments.

5.2. Controls on biogenic export from the euphotic zone

In order to better understand the factors that control the magnitude and timing of the vertical export (i.e. "biologic pump") from the euphotic zone, we examined in detail the relationships among biogenic fluxes at 275 m (trap A) and the temperature and PP of the upper water column. Several important observations are worth noting. For example, we observed a general inverse exponential relationship between $T_{0-25\,m}$ and $PP_{0-100\,m}$ (Fig. 7a). With the exception of two high PP measurements in January 1997 and February 1999 (Table 1), we observed an exponential correlation ($r^2 = 0.4$; $P = 0.05$) between the cooling of the water column due to upwelling and the productivity of the upper ocean (Fig. 7a). This relationship illustrates the upwelling-dominated nature of the Cariaco Basin. Furthermore, during periods when under-trapping is not a problem (see previous discussion), we find that there is a general linear relationship ($r^2 = 0.3$, $P = 0.05$) between the biweekly OC fluxes at 275 m and $PP_{0-100\,m}$ (Fig. 7b). Clearly, some of the scatter in the data is due to the seasonal variability in the phytoplankton and zooplankton compositions, which affect the magnitude and timing of the

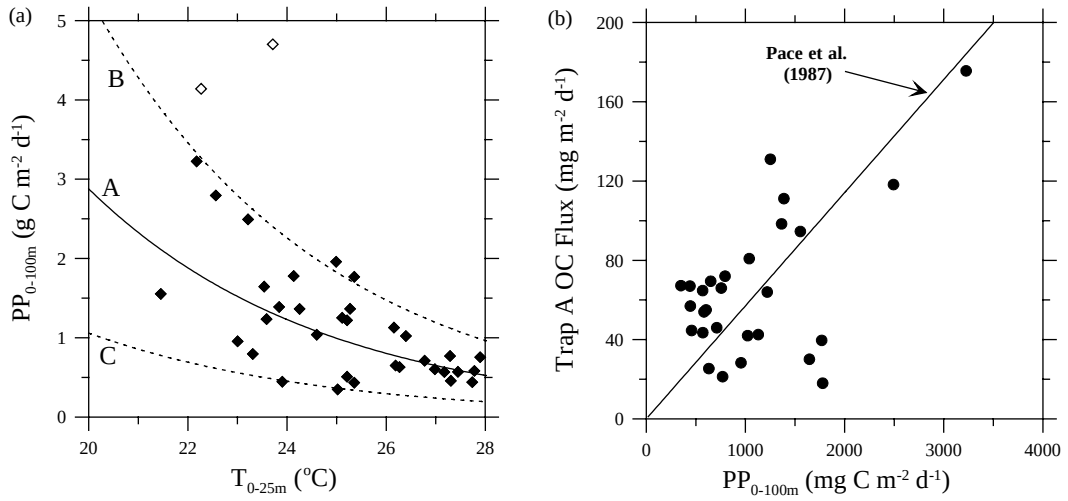

Fig. 7. Graphs of the relationship between (a) average temperature of the top 25 m of the water column ($T_{0-25\,m}$) and integrated water column PP over the top 100 m ($PP_{0-100\,m}$), and (b) $PP_{0-100\,m}$ and organic carbon flux at 275 m. Included in Fig. 7a is the correlation between the two variables (Equation A) as well as two other lines that bracket the variability in the data set (Equations B and C). The line in Fig. 7b represents the expected OC fluxes at 275 m given the measured PP rates (Table 1) according to the empirical relationship developed by Pace et al. (1987).

export flux. Nevertheless, the data fit reasonably well the expression of Pace et al. (1987), which was shown by Thunell et al. (1999) to be the best among others (Suess, 1980; Betzer et al., 1984) at describing OC fluxes measured during the 1995–1996 trap deployment.

Opal fluxes in trap A show a significant positive correlation ($r^2 = 0.8$, $P = 0.05$) with the OC fluxes measured throughout the study period (Fig. 8a). This close relationship between OC and opal fluxes at 275 m depth is to be expected since diatoms are the most significant contributors to the overall PP in the Cariaco Basin and likely account for the majority of carbon export from the euphotic zone (Thunell et al., 2000). $CaCO_3$ fluxes (Fig. 8b) also display a significant positive relationship with OC fluxes albeit with a smaller correlation coefficient ($r^2 = 0.6$, $P = 0.05$). In this case, the weaker correlation is mainly ue to the lower than expected $CaCO_3$ fluxes obtained during the upwelling peaks in 1997 and 1998.

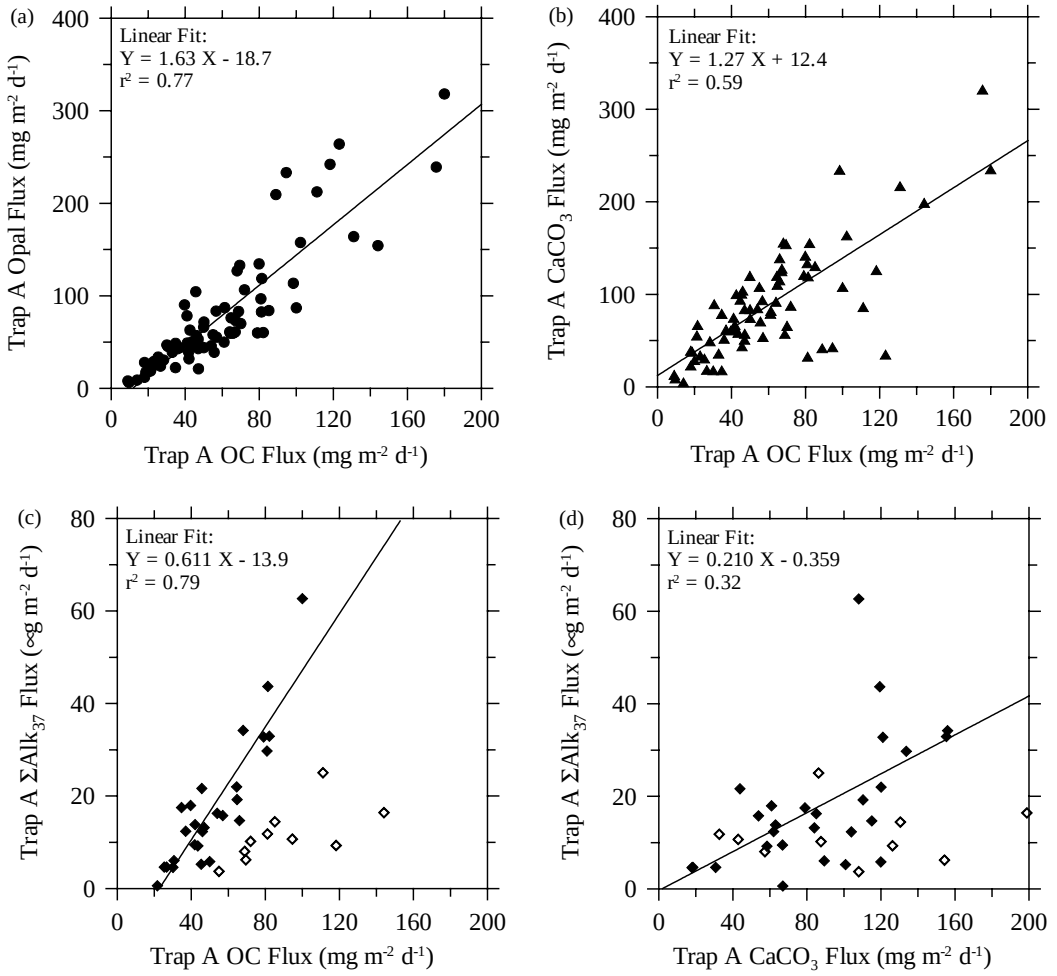

Fig. 8. Correlations between the measured organic carbon (OC) fluxes measured in trap A (275 m) and (a) biogenic opal fluxes, (b) $CaCO_3$ fluxes, and (c) long-chain alkenone (ΣAlk_{37}) fluxes. Also plotted are (d) the correlation between $CaCO_3$ fluxes and ΣAlk_{37} fluxes. The results of the linear fit between the variables are provided in each graph. The open symbols in Figs. 8c and d indicate samples collected at the height of upwelling events during 1997 and 1998, which were not used in the linear correlation calculations. See text for further discussion.

A similar effect is also evident in the plot of long-chain C_{37} alkenone fluxes vs. OC fluxes (Fig. 8c), which shows that ΣAlk_{37} fluxes correlated very well ($r^2 = 0.8$; $P = 0.05$) with OC fluxes throughout most of the study period. However, samples collected during peaks in upwelling (marked with the open symbols in Fig. 8c) during March, July, and November 1997, and March and July 1998 (Fig. 2) deviate from this trend, displaying ΣAlk_{37} fluxes that are lower than expected from the OC fluxes recovered in trap A. These results indicate that during most of the year, alkenone producers contribute a constant fraction of the total organic matter flux exported from the euphotic zone. The major exceptions are periods of maximum upwelling (both during primary and secondary upwelling events), when alkenone contributions are lower than expected either because they account for a smaller fraction of the plankton production or because they contain lower alkenone content. In spite of the general similarities between $CaCO_3$ and ΣAlk_{37} trends in trap A, the correlation between the fluxes of these materials is not very strong (Fig. 8d), suggesting that other sources of $CaCO_3$ (e.g., foraminifers; Tedesco and Thunell, in press) besides haptophyte algae contribute to the carbonate export fluxes in the Cariaco Basin.

5.3. *Annually averaged records of water column fluxes*

In order to correctly use water column fluxes to interpret sedimentary records, it is important to consider the time scales of both measurements, which in the case of the Cariaco Basin sediments include annual varves (Black et al., 1999; Hughen et al., 1996b). Hence, it is useful to examine the annual average fluxes of biogenic materials collected at the three sediment trap depths in the context of the inter-annual variability in hydrographic and productivity conditions of the upper water column. However, because of the possibility of under-trapping or partial clogging discussed above, the annual totals calculated from the data in Fig. 3 may not be truly representative of the fate of particle-bound OC, opal, $CaCO_3$, and ΣAlk_{37} in the Cariaco Basin. For that reason, we have recalculated the total fluxes of these materials in all three traps to exclude those periods during which the TM fluxes at trap B exceeded those measured in trap A (Fig. 9). The annual 1996–1997 averages also exclude the period between March 28 and May 15, 1997, for which we have no flux data because of trap clogging. In order to maintain consistency in the computation of annual averages, we did not use the PP and temperature data for the periods in which flux data were excluded or non-existent. Although these decisions mean that the annual flux data discussed below are based on incomplete records, we believe this approach removes potential biases due to sampling artifacts and more accurately relates the biogenic flux observations to the hydrographic data.

None of the biogenic materials measured in the shallow trap display a clear positive correlation between their annually averaged fluxes and annually averaged total $PP_{0-100\,m}$ (Fig. 9). In the case of OC (Fig. 9a), the highest fluxes were measured during the least productive year, clearly showing that productivity alone does not control carbon export from the euphotic zone in the Cariaco Basin. In contrast, the annually averaged cumulative fluxes of $CaCO_3$ (Fig. 9c) seem to correlate negatively with productivity, as the least productive upwelling cycle (November 1997–October 1998) yielded the highest trap A $CaCO_3$ flux whereas the smallest $CaCO_3$ export was obtained during the first upwelling cycle, which was the most productive. These findings suggest that the low productivity conditions observed during an El Niño year may favor the production and export of calcite-bearing organisms from the surface waters of the Cariaco Basin.

The annually averaged cumulative opal fluxes from trap A (Fig. 9b), on the other hand, display an inverse relationship with temperature clearly indicating that diatoms favor strong upwelling-conditions. Alkenone export (Fig. 9d) from the euphotic zone (trap A) follows a trend opposite to that of opal, increasing steadily as the annual temperature of the upper water column increases because of reduced upwelling. Such trends suggest that alkenone-producing haptophytes are favored during low upwelling years

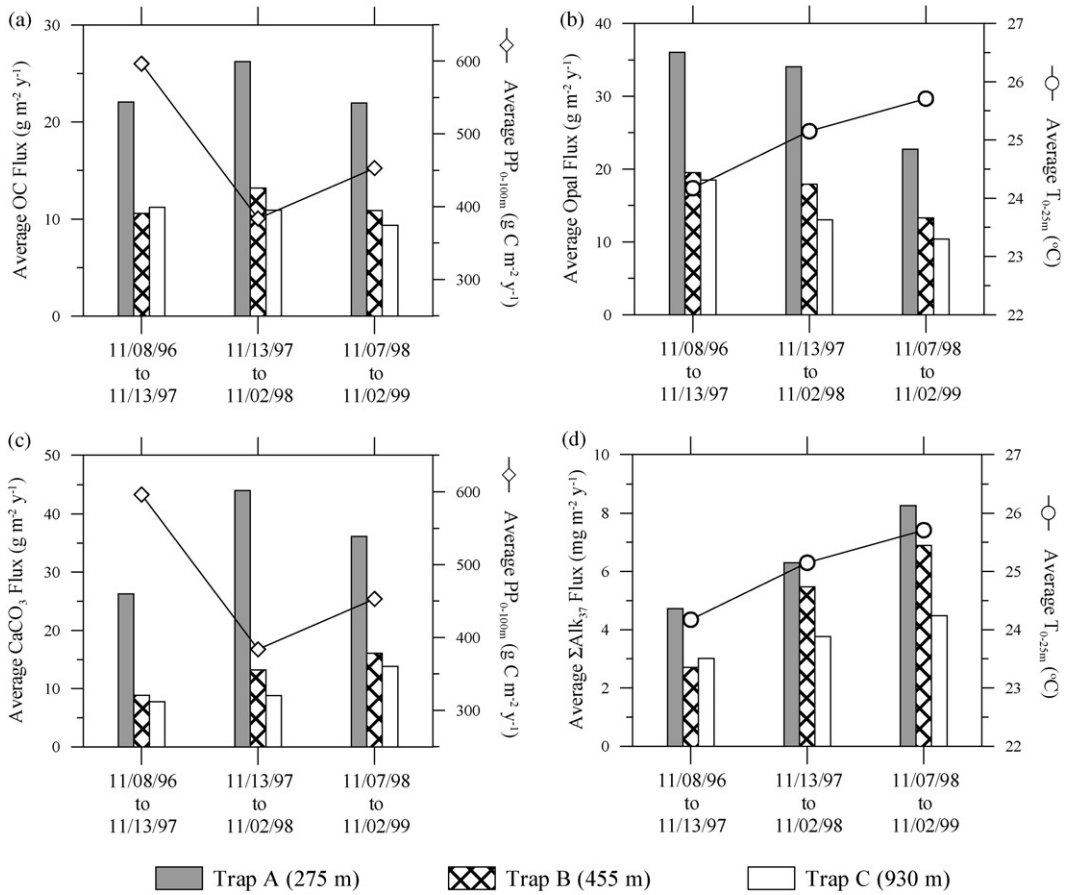

Fig. 9. Annually averaged biogenic fluxes of (a) organic carbon, (b) biogenic opal, (c) $CaCO_3$, and (d) long-chain C_{37} alkenones (ΣAlk_{37}) obtained from traps A, B, and C. The cumulative total fluxes were determined from the mean daily fluxes of each sediment trap deployment (Fig. 3) and combined over each upwelling-stratification cycle (November–October). For this figure, we re-calculated the total fluxes of these materials to exclude those periods between December 97 and February 98, July 98, January to April 99, June 99 (corresponding to trap deployments Car5-05 to Car5-07, Car6-06, Car7-06 to Car7-11, Car7-13, and Car8-02, respectively) during which the TM fluxes at trap B exceeded those measured in trap A (Table 2). Also plotted in the graphs are the annually averaged cumulative PP over the top 100 m of the water column ($PP_{0-100\,m}$) and the annually averaged temperature for the top 25 m of the water column ($T_{0-25\,m}$) for each of the three annual upwelling cycles studied (Table 1). The $PP_{0-100\,m}$ and $T_{0-25\,m}$ data for the periods of under-trapping and trap clogging are excluded from these annual average computations.

and may be negatively correlated with diatom production, perhaps because of competition for light or nutrients. These findings are significant for paleo-reconstructions of plankton production in the Cariaco Basin (e.g., Werne et al., 2000). Although biogenic accumulation rates in sediments may not be direct indicators of past productivity, it appears as if both opal and alkenone sedimentation data may be used to assess past upwelling conditions.

With regards to the reactivity during particle settling through the water column, $CaCO_3$ appears to be the most reactive of the four biogenic materials measured, with 60–70% of the $CaCO_3$ flux measured in trap A being lost by the time it reached trap B (Fig. 9c). The next most reactive materials were OC and opal with ~50% losses between traps A and B and 60% losses between traps A and C (Fig. 9a and b). The least reactive component appeared to be long-chain alkenones

with losses between traps A and B that ranged from 15% to 40% (year 1 and 2, respectively; Fig. 9d). It is important to note, however, that in two of the three annual cycles studied, ΣAlk_{37} losses between traps B and C were considerably higher than those measured for all the other biogenic materials determined. Such a trend indicates that although their export from the euphotic zone is fairly efficient, alkenone degradation continues to occur in the deeper (anoxic) parts of the water column. Notably, the ΣAlk_{37} fluxes in the deeper Cariaco traps (455 and 930 m), which range from 3 to 7 mg m^{-2} yr^{-1} (Fig. 9), are comparable to the mean annual alkenone fluxes measured between 500 and 1000 m depth in other productive regions of the ocean with oxygenated water columns, including the Northeast Pacific (Prahl et al., 1993), the Northwest Pacific (Sawada et al., 1998), the Gulf of California (Goñi et al., 2001), and the Norwegian Sea (Thomsen et al., 1998).

5.4. Sedimentary records of biogenic fluxes

Using the bulk sediment accumulation rates and the concentration data for the various biogenic components (Table 4), we calculated the burial fluxes of OC, opal, $CaCO_3$ and ΣAlk_{37} in the CAR7-2 core (Fig. 10). Because of the uncertainties in the accumulation rates in the top 30 cm of the core, we have chosen to present the burial fluxes only from 1000 to 5500 yr BP at this site. Also included in Fig. 10 for comparison are the average annual sediment trap fluxes for each trap. The dotted line in each of these graphs indicates the water depth of the sediment core to illustrate the expected fluxes at that location.

The rates of OC and opal burial range from 5 to 10 g m^{-2} yr^{-1} and account for ~30% of the water column export fluxes measured in trap A (Fig. 10a and b). Indeed, OC and opal burial fluxes fall between the annual average fluxes determined from the B and C sediment traps, consistent with the relatively good preservation of these materials at the sediment–water interface. The steady decrease in OC and opal accumulation rates with increasing sediment age may be due to either in situ degradation or an overall increase in accumulation rates from 5500 to 1000 yr BP. Nevertheless, the general trends suggest that organic matter inputs and diatom productivity in the Cariaco Basin have remained rather constant during this period and were comparable to present day values. The major exception is the lower opal accumulation rates measured around 1600 yr BP, which is indicative of lower diatom productivity. Overall, the OC burial fluxes at this site are comparable to the values (6–12 g m^{-2} yr^{-1}) measured by Werne et al. (2000) in sediments of similar age from the western side of the Cariaco Basin. The OC burial rates measured in the Cariaco Basin are similar to the value (12 g m^{-2} yr^{-1}) obtained in sediments from the oxygen minimum zone (650 m depth) of the Gulf of California (Goñi et al., 2001), another upwelling-dominated region. For comparison, McCaffrey et al. (1990) measured OC accumulation rates of 40 g m^{-2} yr^{-1} in sediments from 250 m water depth within the upwelling region off Peru.

In contrast to OC and opal, the $CaCO_3$ burial fluxes range from 30 to 60 g m^{-2} yr^{-1} and are comparable to the water column fluxes measured in trap A, significantly exceeding the values recorded in traps B and C (Fig. 10c). These results reinforce our interpretation that post-collection processes may bias the $CaCO_3$ fluxes measured in the deeper traps, which might not be representative of the input to the underlying sediments. Nevertheless, as was the case of both OC and opal, the general down core decrease in $CaCO_3$ accumulation rates can be interpreted either as in situ degradation or an overall increase in $CaCO_3$ inputs from 5000 to 1000 yr BP. There is a minimum in $CaCO_3$ burial between 1600 and 1800 yr BP that is coincident with the low opal burial rates (Fig. 10b) and a peak at 2600 yr BP, all of which indicate $CaCO_3$ inputs have varied during this period. As with OC, our measurements agree very well with the $CaCO_3$ burial fluxes (~40 g m^{-2} yr^{-1}) determined by Werne et al. (2000). In that paper, the $CaCO_3$ data was originally mislabeled as inorganic carbon.

The burial fluxes of ΣAlk_{37} in CAR7-2 range from 0.5 to 1.8 mg m^{-2} yr^{-1} and represent ~10% of the export flux measured in trap A (Fig. 10d). Notably, the C_{37} alkenone fluxes measured in this study are somewhat lower than the rates

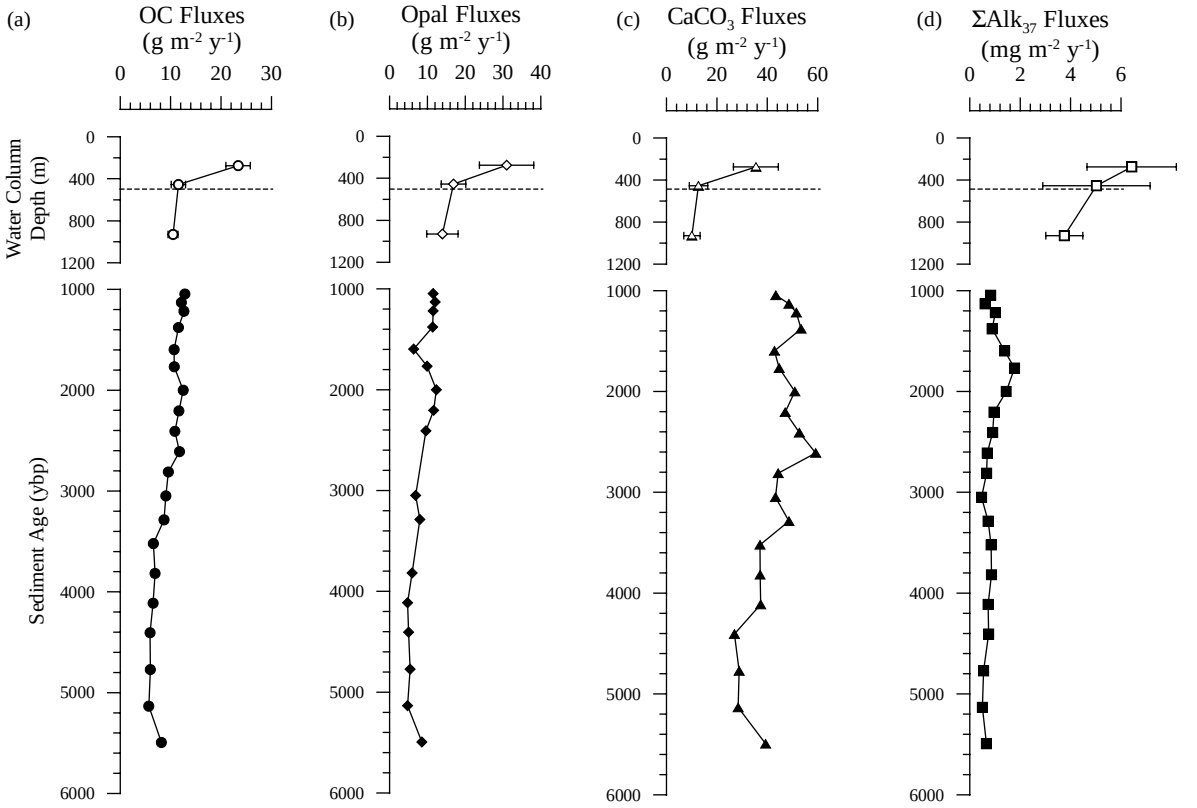

Fig. 10. Average water column fluxes and sediment burial fluxes of (a) organic carbon, (b) biogenic opal, (c) $CaCO_3$ and (d) long-chain C_{37} alkenones determined from the 3-year sediment trap study and the sediments from CAR7-2. The average fluxes of the 3 upwelling cycles from each trap are plotted vs. water column depth for each biogenic material in the top part of the figure. The dotted line in each of these graphs indicates the water column depth of the sediment core in order to illustrate the expected fluxes arriving at this location (Fig. 1). In the case of sediment burial fluxes, the data plotted exclude the top 30 cm of the gravity core, which were disturbed during collection. The burial fluxes are plotted vs. the sediment age of each horizon as determined from the age model for the core (Black et al., 2001).

($5\,mg\,m^{-2}\,yr^{-1}$) reported by Werne et al. (2000) for the western side of the basin. There was an error in the units of the fluxes reported in their original paper that we corrected in order to make this comparison. For comparison, ΣAlk_{37} accumulation fluxes in other low oxygen environments underneath zones of active upwelling range from $5\,mg\,m^{-2}\,yr^{-1}$ in 650 m deep sediments from the Gulf of California (Goñi et al., 2001) to $14\,mg\,m^{-2}\,yr^{-1}$ in 250 m deep sediments from the Peru upwelling margin (McCaffrey et al., 1990).

Unlike any of the other materials measured (Fig. 10), the rates of ΣAlk_{37} burial in Cariaco Basin sediments are markedly lower than the fluxes measured in all traps, indicating that alkenones are lost very efficiently once they reach the sediments. Such large flux attenuation upon burial is expected from the high reactivity exhibited by most algal lipids at the sediment water-interface (e.g., Wakeham et al., 2002; Müller and Fischer, 2001; Prahl et al., 2000), which also appears to be the case for the anoxic conditions characteristic of this site. The diagenetic reactions that may be responsible for these trends include direct anaerobic degradation as well as the formation of sulfur–carbon bridges at unsaturated sites of individual alkenones. This latter process, often referred to as natural sulfurization, results in

the removal of unsaturated lipids from the analytical window of most extraction and chromatographic procedures (e.g., Kohnen et al., 1989; de Graaf et al., 1992), which can be interpreted as an apparent flux loss. Further work is needed to evaluate the quantitative importance of these reactions on the alkenone geochemistry of the study site (e.g., Prahl et al., 1996). Hence, our results imply that caution must be used in the quantitative interpretation of burial fluxes in Cariaco Basin sediments, as the diagenetic processes near the sediment–water interface significantly alter the productivity signals arriving from the overlying water column.

In spite of the diagenetic imprinting evident in the sediment compositions, it is important to note that this low resolution sediment record exhibits a marked peak in the ΣAlk_{37} burial fluxes around 1600–1800 yr BP that coincides with minima in opal and $CaCO_3$ burial fluxes. Qualitatively, we can conclude that these measurements are consistent with lower diatom productivity and enhanced alkenone-bearing haptophyte production at this time. Based on the trends obtained from the 3-year sediment trap study, we can speculate that such compositions may be indicative of lower upwelling conditions, such as the ones we measured during the 1998–1999 upwelling cycle, which resulted in elevated ΣAlk_{37} water column fluxes and diminished opal fluxes. Clearly, this preliminary interpretation is based on a rather limited (three annual cycles) set of sinking flux observations. Longer sediment trap records and better constraints in the degradation behavior of these compounds near the sediment–water interface are needed in order to draw more quantitative conclusions about the sedimentary record.

5.5. Concluding remarks

The results from the first three complete years of sediment trap collection in the on-going CARIACO project show several important seasonal and inter-annual trends in the export of biogenic materials from the euphotic zone that are closely tied to the upwelling regime and PP of the upper water column. These trends illustrate the variability in the composition and productivity of the food web in the Cariaco Basin and may be used to better reconstruct past conditions from the sedimentary record. However, as shown by our work, both the transport of these materials through the water column and their preservation in the underlying sediments are often accompanied by significant changes in the magnitude and composition of the export fluxes. These changes must be understood before further insight into the paleoceanography of the Cariaco Basin can be gained. A critical aspect that needs further attention is the cycling of biogenic materials near the sediment–water interface, where many of the reactions responsible for the contrasts between sediment trap and burial fluxes occur. We are currently conducting such a study focused on the collection and analyses of undisturbed surface sediments from the Cariaco Basin. Furthermore, we are continuing the sediment trap time-series in order to obtain a longer record that would allow us to better explore the inter-annual contrasts in hydrography, productivity and biogenic fluxes in this area.

Acknowledgements

We thank the personnel from the Estación de Investigaciones Marinas de la Fundación La Salle for logistical support and the crew of the Buque Oceanográfico Hermano Ginés for their invaluable assistance at sea. This paper benefited from three anonymous reviews, discussions with fellow CARIACO scientists, including Mary Scranton, Gordon Taylor, Mark Woodworth, and comments by Liz Gordon. Funding for this research was provided by the National Science Foundation (OCE 9729697 and OCE 0118349 to Thunell and Goni, and OCE 9729284 to Muller-Karger) and the Consejo Nacional de Investigaciones Científicas y Tecnológicas (CONICIT, Venezuela, grant 96280221).

References

Andrade, C.A., Barton, E.D., 2000. Eddy development and motion in the Caribbean Sea. Journal of Geophysical Research 105, 191–201.

Astor, Y., Muller-Karger, F., Scranton, M., 2003. Seasonal and interannual variation in the hydrography of the Cariaco Basin: implications for basin ventilation. Continental Shelf Research 23, 125–144.

Baker, E.T., Milburn, H.B., Tennant, D.A., 1988. Field assessment of sediment trap efficiency under varying flow conditions. Journal of Marine Research 46, 573–592.

Betzer, P., Showers, W., Laws, E., Winn, C., DiTullio, G., Kroopnik, P., 1984. Primary production and particle fluxes on a transect of the equator at 153°W in the Pacific Ocean. Deep-Sea Research 31, 1–11.

Black, D.E., Peterson, L.C., Overpeck, J.T., Kaplan, A., Evans, M.N., Kashgarian, M., 1999. Eight centuries of North Atlantic Ocean atmosphere variability. Science 286, 1709–1713.

Black, D.E., Thunell, R.C., Kaplan, A., Tedesco, K.A., Tappa, E.J., Peterson, L.C., 2001. Late Holocene tropical Atlantic climate variability: records from the Cariaco Basin. EOS Transactions, AGU, 82, Fall Meeting Abstracts PP22B-01.

Buesseler, K.O., 1991. Do upper-ocean sediment traps provide an accurate record of particle flux? Nature 353, 420–423.

Chavez, F.P., Strutton, P.G., Friedrich, G.E., Feely, R.A., Feldman, G.C., Foley, D.G., McPhaden, M.J., 1999. Biological and chemical response of the equatorial Pacific Ocean to the 1997–98 El Niño. Science 286, 2126–2131.

de Graaf, W., Sinninghe, J.S., de Leeuw, J.W., 1992. Laboratory simulation of natural sulphurization: I. Formation of monomeric and oligomeric isoprenoid polysulphides by low-temperature reactions of inorganic polysusphides with phytol and phytadienes. Geochimica et Cosmochimica Acta 56, 4321–4328.

Deuser, W.G., 1973. Cariaco Trench: oxidation of organic matter and residence time of anoxic water. Nature 242, 601–603.

Froelich, P.N., 1980. Analysis of organic carbon in marine sediments. Limnology and Oceanography 25, 565–572.

Goñi, M.A., Hartz, D.M., Thunell, R.C., Tappa, E., 2001. Oceanographic considerations for the application of the alkenone-based paleotemperature $U^{K'}_{37}$ index in the Gulf of California. Geochimica et Cosmochimica Acta 65, 545–557.

Haug, G., Pedersen, T., Sigman, D., Calvert, S, Nielsen, B., Peterson, L., 1998. Glacial/interglacial: variations in production and nitrogen fixation in the Cariaco Basin during the last 580 kyr. Paleoceanography 13, 427–432.

Herrera, L.E., Febres-Ortega, G., 1975. Procesos de surgencia y de renovacion de aquas en la Fosa de Cariaco, Mar Caribe. Boletín Instituto Oceanográfico Universidad de Oriente 14, 31–44.

Honjo, S., Doherty, K., 1988. Large-aperture time series oceanic sediment traps: design objectives, construction and application. Deep-Sea Research 35, 133–149.

Hughen, K.A., Overpeck, J.T., Peterson, L.C., Trumbore, S., 1996a. Rapid climate changes in the tropical Atlantic region during the last deglaciation. Nature 380, 51–54.

Hughen, K.A., Overpeck, J.T., Peterson, L.C., Anderson, R.F., 1996b. The nature of varved sedimentation in the Cariaco Basin, Venezuela, and its paleoclimatic significance. In: Kemp, A.E.S. (Ed.), Palaeoclimatology and Palaeoceanography from Laminated Sediments. Geological Society Special Publication No. 116, London, pp. 171–183.

Hughen, K.A., Overpeck, J.T., Lehman, S.J., Kashgarian, M., Southon, J., Peterson, L.C., Alley, R., Sigman, D.M., 1998. Deglacial changes in ocean circulation from an extended radiocarbon calibration. Nature 391, 65–68.

Hughen, K., Southon, J., Lehman, S., Overpeck, J., 2000. Synchronous radiocarbon and climate shifts during the last deglaciation. Science 290, 1951–1954.

Kohnen, M.E.L., Sinninghe Damste, J.S., ten Haven, H.L., de Leeuw, J.W., 1989. Early incorporation of polysulphides in sedimentary organic matter. Nature 341, 640–641.

Lidz, L., Charm, W.B., Ball, M.M., Valdes, S., 1969. Marine basins off the coast of Venezuela. Bulleting of Marine Science 19, 1–17.

Marlowe, I.T., Brassell, S.C., Eglinton, G., Green, J.C., 1984. Long chain unsaturated ketones and esters in living algae and marine sediments. Organic Geochemistry 6, 135–141.

McCaffrey, M.A., Farrington, J.W., Repeta, D.J., 1990. The organic geochemistry of Peru margin surface sediments: I. A comparison of the C37 alkenone and historical El Niño records. Geochimica et Cosmochimica Acta 54, 1671–1682.

Morrison, J.M., Nowlin Jr., W.D., 1982. General distributions of water masses within the eastern Caribbean Sea during winter of 1972 and fall of 1983. Journal of Geophysical Research 87, 4207–4229.

Morrison, J.M., Smith, O.P., 1990. Geostrophic transport variability along the Aves Ridge in the eastern Caribbean Sea during 1985–1986. Journal of Geophysical Research 95, 699–710.

Mortlock, R., Froelich, P., 1989. A simple method for the rapid determination of biogenic opal in pelagic marine sediments. Deep-Sea Research 36, 1415–1426.

Müller, P.J., Fischer, G., 2001. A 4-year sediment trap record of alkenones from the filamentous upwelling region off Cape Blanc, NW Africa and a comparison with distributions in underlying sediments. Deep-Sea Research I 48, 1877–1903.

Muller-Karger, F.E., Aparicio-Castro, R., 1994. Mesoscale processes affecting phytoplankton abundance in the southern Caribbean Sea. Continental Shelf Research 14, 199–221.

Muller-Karger, F., Varela, R., Thunell, R., Scranton, M., Bohrer, R., Taylor, G., Capelo, J., Astor, Y., Tappa, E., Ho, T.-Y., Walsh, J.J., 2001. Annual cycle of primary production in the Cariaco Basin: response to upwelling and implications for vertical export. Journal of Geophysical Research 106, 4527–4542.

Ostermann, D.R., Karbott, D., Curry, W.B., 1990. Automated system to measure the carbonate concentration of sediments. WHOI Technical Report No. 90-03.

Overpeck, J., Peterson, L., Kipp, N., Rind, D., 1989. Climate change in the circum-North Atlantic region during the last deglaciation. Nature 338, 553–557.

Pace, M., Knauer, G., Karl, D., Martin, J., 1987. Primary production, new production and vertical flux in the eastern Pacific Ocean. Nature 325, 803–804.

Pauluhn, A., Chao, Y., 1999. Tracking eddies in the subtropical north-western Atlantic Ocean. Physics and Chemistry of the Earth 24, 415–421.

Peterson, L.C., Overpeck, J.T., Kipp, N.G., Imbrie, J., 1991. A high-resolution late quaternary upwelling record from the anoxic Cariaco Basin, Venezuela. Paleoceanography 6, 99–119.

Peterson, L., Haug, G., Hughen, C., Rohl, U., 2000. Rapid changes in the hydrologic cycle of the tropical Atlantic during the last glacial. Science 290, 1947–1951.

Prahl, F.G., Collier, R.B., Dymond, J., Lyle, M., Sparrow, M.A., 1993. A biomarker perspective on prymnesiophyte productivity in the northeast Pacific Ocean. Deep-Sea Research I 40, 2061–2076.

Prahl, F.G., Pinto, L.A., Sparrow, M.A., 1996. Phytane from chemolytic analysis of modern marine sediments: a product of desulfurization or not? Geochimica et Cosmochimica Acta 60, 1065–1073.

Prahl, F.G., Dymond, J., Sparrow, M.A., 2000. Annual biomarker record for export production in the central Arabian Sea. Deep-Sea Research II 47, 1581–1604.

Reimers, C.E., Ruttenberg, K.C., Canfield, D.E., Christianses, M.B., Martin, J.B., 1996. Porewater pH and authigenic phases formed in the uppermost sediments of the Santa Barbara Basin. Geochimica et Cosmochimica Acta 60, 4037–4057.

Richards, F.A., 1975. The Cariaco Basin (Trench). Oceanography and Marine Biology-Annual Review 13, 11–67.

Rosell-Melé, A., Carter, J., Parry, A., Eglinton, G., 1995. Determination of the UK'37 index in geological samples. Analytical Chemistry 67, 1283–1289.

Sawada, K., Handa, N., Nakatsuka, T., 1998. Production and transport of long-chain alkenones and alkyl alkenoates in a sea water column in the northwestern Pacific off central Japan. Marine Chemistry 59, 219–234.

Scholten, J.C., Fietzke, J., Vogler, S., Rutgers van del Loeff, M.M., Mangini, A., Koeve, W., Waniek, J., Stoffers, P., Antia, A., Kuss, J., 2001. Trapping efficiencies of sediment traps from the deep Eastern North Atlantic: the ^{230}Th calibration. Deep-Sea Research II 48, 2383–2408.

Scranton, M.I., Astor, Y., Bohrer, R., Ho, T.-Y., Muller-Karger, F.E., 2001. Controls on temporal variability of the geochemistry of the deep Cariaco Basin. Deep-Sea Research I 48, 1605–1625.

Sholkovitz, E., 1973. Interstitial water chemistry of the Santa Barbara Basin sediments. Geochimica et Cosmochimica Acta 37, 2043–2073.

Stuiver, M., Braziunas, T.F., 1993. Modeling atmospheric ^{14}C influences and ^{14}C ages of marine samples to 10,000 BC. Radiocarbon 34, 137–189.

Suess, E., 1980. Particulate organic carbon flux in the oceans—surface productivity and oxygen utilization. Nature 228, 260–263.

Taylor, G.T., Iabichella, M., Ho, T.-Y., Scranton, M.I., Thunell, R.C., Muller-Karger, F., Varela, R., 2001. Chemoautotrophy in the redox transition zone of the Cariaco Basin: a significant midwater source of organic carbon production. Limnology and Oceanography 46, 148–163.

Tedesco, K.A., Thunell, R.C. Seasonal and interannual variations in planktonic foraminiferal flux and assemblage composition in the Cariaco Basin, Venezuela. Journal of Foraminiferal Research, in press.

Thomsen, C., Shulz-Bull, D.E., Petrick, G., Duinker, J.C., 1998. Seasonal variability in the long-chain alkenone flux and the effect on the Uk37-index in the Norwegian Sea. Organic Geochemistry 28, 311–323.

Thunell, R., Tappa, E., Varela, R., Llano, M., Astor, Y., Muller-Karger, F., Bohrer, R., 1999. Increased marine sediment suspension and fluxes following an earthquake. Nature 398, 233–236.

Thunell, R.C., Varela, R., Llano, M., Collister, J., Muller-Karger, F., Bohrer, R., 2000. Organic carbon fluxes, degradation, and accumulation in an anoxic basin: sediment trap results from the Cariaco Basin. Limnology and Oceanography 45, 300–308.

United Nations Educational, Scientific, and Cultural Organization (UNESCO), Protocols for the Joint Global Ocean Flux Study (JGOFS) core measurements, 1994. In: IOC Manuals and Guides, Vol. 29, Paris, pp. 128–140.

Volkman, J.K., Eglinton, G., Corner, E.D.S., Forsberg, T.E.V., 1980. Long-chain alkenes and alkenones in the marine coccolithophorids *Emiliania huxleyi*. Phytochemistry 19, 2619–2622.

Volkman, J.K., Barrett, S.M., Blackburn, S.I., Sikes, E.L., 1995. Alkenones in *Gephyrocapsa oceanica*: implications for studies of paleoclimate. Geochimica et Cosmochimica Acta 59, 513–520.

Wakeham, S.G., Peterson, M.L., Hedges, J.I., Lee, C., 2002. Lipid biomarker fluxes in the Arabian Sea, with a comparison to the equatorial Pacific Ocean. Deep-Sea Research II 49, 2265–2301.

Walsh, J.J., Dieterle, D.A., Muller-Karger, F.E., Bohrer, R., Bisset, W.P., Varela, R.J., Aparicio, R., Díaz, R., Thunell, R., Taylor, G.T., Scranton, M.I., Fanning, K.A., Peltzer, E.T., 1999. Simulation of carbon–nitrogen cycling during spring upwelling in the Cariaco Basin. Journal of Geophysical Research 104, 7807–7825.

Werne, J.P., Hollander, D.J., Lyons, T.W., Peterson, L.C., 2000. Climate-induced variations in productivity and planktonic ecosystem structure from the Younger Dryas to Holocene in the Cariaco Basin, Venezuela. Paleoceanography 15, 19–29.

Yu, E.-F., Francois, R., Bacon, M.P., Honjo, S., Fleer, A.P., Manganini, S.J., Rutgers van der Loeff, M.M., Ittekot, V., 2001. Trapping efficiency of bottom-tethered sediment traps estimated from the intercepted fluxes of ^{230}Th and ^{231}Pa. Deep-Sea Research I 48, 865–889.